

Open-World Panoptic Segmentation

Matteo Sodano

Federico Magistri

Jens Behley

Cyrill Stachniss

Abstract—Perception is a key building block of autonomously acting vision systems such as autonomous vehicles. It is crucial that these systems are able to understand their surroundings in order to operate safely and robustly. Additionally, autonomous systems deployed in unconstrained real-world scenarios must be able of dealing with novel situations and object that have never been seen before. In this article, we tackle the problem of open-world panoptic segmentation, i.e., the task of discovering new semantic categories and new object instances at test time, while enforcing consistency among the categories that we incrementally discover. We propose Con2MAV, an approach for open-world panoptic segmentation that extends our previous work, ContMAV, which was developed for open-world semantic segmentation. Through extensive experiments across multiple datasets, we show that our model achieves state-of-the-art results on open-world segmentation tasks, while still performing competitively on the known categories. We will open-source our implementation upon acceptance. Additionally, we propose PANIC (Panoptic ANomalies In Context), a benchmark for evaluating open-world panoptic segmentation in autonomous driving scenarios. This dataset, recorded with a multi-modal sensor suite mounted on a car, provides high-quality, pixel-wise annotations of anomalous objects at both semantic and instance level. Our dataset contains 800 images, with more than 50 unknown classes, i.e., classes that do not appear in the training set, and 4000 object instances, making it an extremely challenging dataset for open-world segmentation tasks in the autonomous driving scenario. We provide competitions for multiple open-world tasks on a hidden test set. Our dataset and competitions are available at <https://www.ipb.uni-bonn.de/data/panic>.

1 INTRODUCTION

INTERPRETING sensor data is a key capability needed by autonomous vision systems operating in unconstrained real-world scenarios. Such systems must be able to understand their surroundings to operate safely and robustly. For this reason, we witnessed enormous progress in scene interpretation tasks such as object detection [24], [66], semantic segmentation [48], [53], instance segmentation [28], [50], and panoptic segmentation [13], [38], [67], [74]. However, these tasks in their conventional setting share the limiting assumption that all classes and objects that appear at inference time have already been seen at training time. This so-called *closed-world* assumption greatly limits the deployment of such algorithms in the real world. A central challenge for learning-based systems is the ability to deal with something that they have never seen before at training time. For example, autonomous cars navigating in the real world will eventually experience situations and objects that they have not seen before, and need to be able to identify them in order to operate safely and not cause any harm. Thus, autonomous vision systems should be able to deal with the *open-world* scenario, i.e., the fact that not everything can be covered in the training data and novel objects and categories should be identified at test time.

In the past, we witnessed that the availability of high-quality publicly-available datasets [16], [44], [84] has contributed to the progress in semantic scene understanding tasks. Deep learning algorithm, based on convolutional neural networks and transformers, yield outstanding results on these datasets [12], [13], [76], but they typically work under the closed-world assumption, being only able to provide predictions for a closed set of known categories. Such systems cannot recognize an object that belongs to none of the known categories, and they tend to be overconfident and

assign such an object to one of the known classes. However, the capability of identifying unknown objects and classes is of primal importance for perception, and motivated the creation of anomaly benchmarks such as Fishyscapes [7], CAOS [30], or SegmentMeIfYouCan [10]. However, issues such as the limited variability of objects (in Fishyscapes and SegmentMeIfYouCan), the use of synthetic images (in Fishyscapes and CAOS), the lack of a public benchmark (CAOS), or the absence of objects and semantic classes to address only a binary segmentation among anomalous areas and known areas (SegmentMeIfYouCan), hampers a proper evaluation for open-world semantic interpretation tasks.

In this article, we propose Con2MAV, a novel method for open-world panoptic segmentation. It jointly addresses anomaly segmentation, open-world semantic and open-world panoptic segmentation, and achieves state-of-the-art results on several public datasets, such as SegmentMeIfYouCan [10], COCO [44], BDDAnomaly from CAOS [30], and SUIM [35]. Examples of Con2MAV predictions are shown in Fig. 1

Additionally, driven by the several great works recently published in the open-world domain [17], [26], [56], [65], [75], we propose the PANIC (Panoptic Anomalies In Context) benchmark in order to tackle open-world segmentation tasks. We recorded our dataset in the streets of Bonn, Germany, with a sensor suite [79] mounted on top of a vehicle, and manually annotated all anomalous objects in the image with their semantic category and instance, in order to allow tasks spanning from anomaly segmentation to open-world semantic and panoptic segmentation. We provide 800 images, split into validation and hidden test set, i.e., there is no ground truth annotation released for the test set. We consider objects that do not appear in Cityscapes [16] as anomalous. They can appear anywhere in the image and have any size. Additionally, no unknown class that appears in the test set is also present in the validation set, making the test set truly hidden. Examples from the dataset are shown in Fig. 2.

Con2MAV is an extension of our previous approach [75], ContMAV, presented at CVPR 2024. ContMAV is a fully convolutional neural network for open-world semantic segmentation. Specifically, we introduced a novel loss function that allowed us

- M. Sodano, F. Magistri, and J. Behley are with the Center for Robotics, University of Bonn, Germany. E-mails: {matteo.sodano, federico.magistri, jens.behley}@igg.uni-bonn.de
- C. Stachniss is with the Center for Robotics, University of Bonn, Germany, and the Lamarr Institute for Machine Learning and Artificial Intelligence, Germany. E-Mail: cyrill.stachniss@igg.uni-bonn.de

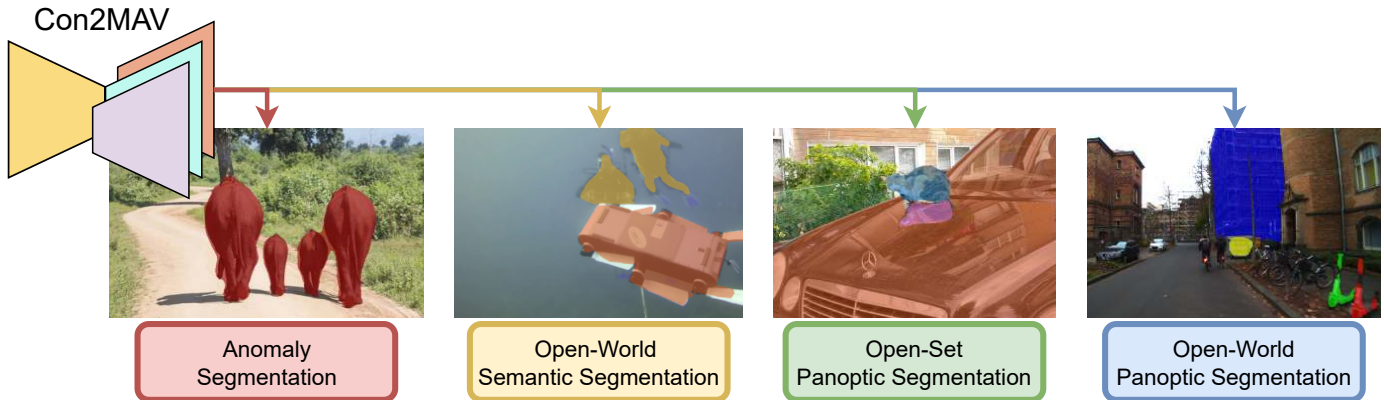


Fig. 1. Our proposed approach, Con2MAV, is able to tackle multiple open-world tasks and segment unknown objects and categories in multiple datasets spanning multiple domains. In the figure, we show predictions on SegmentMeIfYouCan [10] for anomaly segmentation, SUIM [35] for open-world semantic segmentation, COCO [44] for open-set panoptic segmentation, and PANIC (ours) for open-world panoptic segmentation (we show only the instance mask for clarity). We show further qualitative examples in Sec. 6 and in the supplementary material.

to distinguish among different novel classes by building a unique class descriptor for each known (at training time) and unknown (at test time) category. With Cont2MAV here, instead, we modify the main architecture in order to address the main limitations of the previous approach. Most importantly, we introduce a new decoder to segment individual instances, which is not possible with our previous approach. Additionally, ContMAV has a few limitations. Specifically, it relies on several manually-tuned thresholds for predicting the final anomaly scores, and it performs poorly when the training dataset has few known categories, because the class descriptor we aim to build for the unknown classes is not representative enough. Here, we overcome these limitations, as most of the thresholds are now implicitly derived from the formulation of the approach, and we fix the dimension of the class descriptor as we build it before the last convolution of the network. Furthermore, in our previous work we reported experiments on two datasets, namely BDDAnomaly [30] and SegmentMeIfYouCan [10]. In this article, we additionally report experiments on COCO [44] and SUIM [35], as well as our proposed dataset designed specifically for open-world segmentation tasks.

Lastly, we provide an extended discussion on open-world tasks. Beside anomaly segmentation, which is quite common in the literature, other open-world tasks suffer from an ambiguous task nomenclature, and it is not rare to encounter different works addressing the same task but using a different name. Here, we try to overcome this problem and aim to unify the nomenclature for open-world tasks, hoping that this would make open-world segmentation more common and accessible in the future.

In sum, our contributions are the following:

- We propose a fully convolutional neural network that achieves state-of-the-art performance on open-world segmentation tasks, extending ContMAV in order to predict also instances and not only semantic categories, while still providing compelling closed-world performance in Sec. 4.
- We improve our previous approach, ContMAV, addressing its main limitations of (a) having several thresholds to manually tune, and (b) not being able to find novel classes when too few known classes are used for training.
- We provide a dataset, called PANIC, with 800 images with pixel-wise annotations of more than 50 anomalous classes and more than 4000 object instances, with public

competitions for several open-world segmentation tasks in Sec. 5.

- We propose a non-ambiguous nomenclature for common open-world segmentation tasks, overcoming the issue of using different names for the same task, as we believe that unifying the technical terms makes the tasks more distinct and recognizable in Sec. 3.

2 RELATED WORK

Recently, semantic and panoptic segmentation have been among the most prominent perception tasks in different domains, such as autonomous driving [8], [52], [53], [81], indoor navigation [32], [41], [74], and agricultural robotics [15], [50], [54], [67]. However, they mostly operate in closed-world settings, while the open-world domain has been relatively under-explored until recently.

Open-World Detection and Segmentation. The first approaches that aimed to relax the closed-world assumption in order to identify previously-unseen samples targeted the problem of anomaly detection and classification. Mostly, their goal was to identify and discard anomalous samples. Early approaches rely on modification of standard closed-world segmentation techniques, such as using an extra class for identifying everything anomalous [7], [55], [78], thresholding or modifying the softmax activation [4], [9], [31], and using model ensembles [42], [80]. These approaches paved the way for modern open-world segmentation techniques, despite having issues in reliably identifying anomalies, due to the fact that usually the predictions were overconfident and showed a peak in the softmax activations also for unknown samples [60], [77]. Later on, researchers explored novel ideas for segmenting unknowns, such as maximizing entropy [19], predicting energy scores [46], and estimating the model uncertainty via Bayesian deep learning [21], [42], [72] or the network gradients [45], [49]. Many recent approaches [34], [85] instead, rely on having some unknown objects in the training set, to be able to distinguish the known objects from all others. Recently, open-world segmentation is gaining traction and many promising approaches came to light. Most novel approaches predict the anomalous area and cluster individual instances in a class-agnostic fashion [22], [56], [57], [65]. Discovering multiple unknown semantic classes is, instead, a relatively unexplored research direction [75].

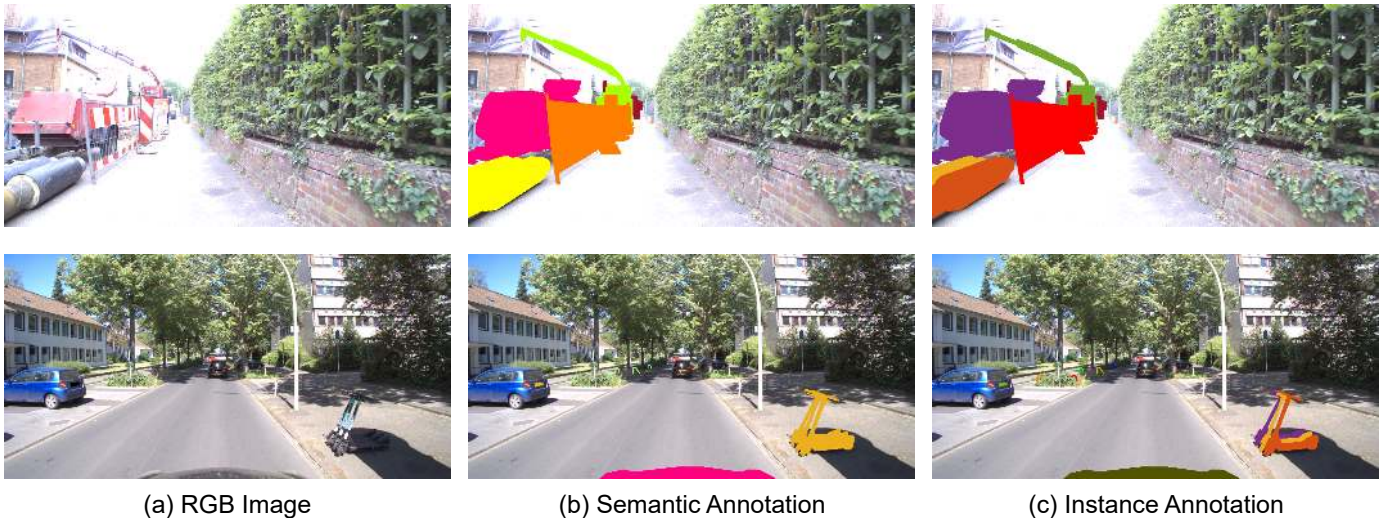


Fig. 2. Our dataset, PANIC, provides pixel-wise annotations of unknown semantic categories and object instances of RGB images. The images have been recorded with a sensor suite [79] mounted on a vehicle driving in Bonn, Germany. The dataset consists of images collected at different times of day over the span of more than a year, and more than 50 different unknown classes appear that are not present in Cityscapes.

Alternative techniques for discovering new objects have also been explored. Generative models [40], [92] have proven useful for this task, since in the reconstruction phase unknown areas will have a lower reconstruction quality than the known areas, and can thus be recognized by looking at the most dissimilar areas between the input and the output.

A similar but inherently different research direction is represented by the open-vocabulary setting. This family of approaches leverages large-scale visual-language models such as CLIP [64] and ALIGN [36] to discover new semantic categories with the help of a text prompt [23], [43], [63], [86], [90].

In this paper, we present a fully convolutional neural network for open-world panoptic segmentation. Our goal is to be able to find multiple unknown semantic categories, and segment individual objects within each one of them. Furthermore, we do not rely on unknown objects in the training set, nor use techniques such as generative models or visual-language models.

Datasets. While large-scale datasets exist for closed-world segmentation in different domains [16], [44], [84], datasets for open-world segmentation are comparably rare. The WildDash dataset [89] provides anomalous images where full-image anomalies are present. Another dataset is MVTEC [5], that mostly targets the industrial scenario. BrainMRI & HeadCT [71] are two datasets targeting the medical domain for detecting lesions on different organs. Among the most common datasets for open-world segmentation in the autonomous driving domain are the Fishyscapes-LostAndFound benchmark [6], [62], which is based on the same setup as Cityscapes and presents anomalous objects in the middle of the street, the CAOS benchmark [30] that originates from the BDD100K [88] dataset to create an open-world test set, and TAO-OW [47] for open-world tracking. These datasets are, however, characterized by a low diversity of anomalies. Chan et al. [10] introduced the SegmentMeIfYouCan benchmark, which is a test set that relies on the known classes from Cityscapes and introduces anomalies of various kinds and sizes. However, it provides a limited number of images, and no semantic nor instance annotation, but only a binary segmentation mask between known and unknown. Recently, Nekrasov et al. [58] extended SegmentMeIfYouCan by adding instance information, even though

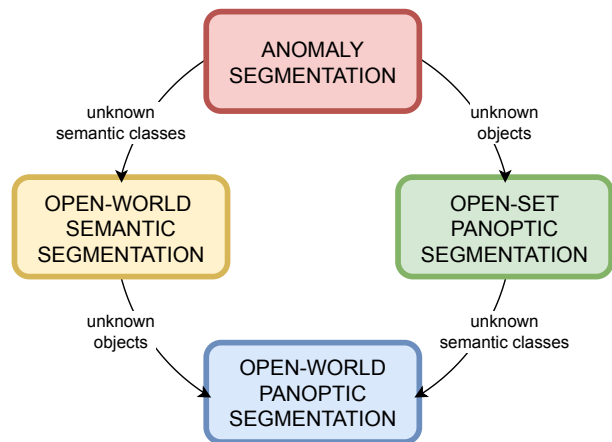


Fig. 3. A schematic breakdown of the task discussed in this paper.

semantic information is still missing.

In this work, we propose a dataset for open-world panoptic segmentation with more than 50 unknown classes and more than 4000 instances. We assume everything that appears in Cityscapes to be known, and provide pixel-wise annotations for the unknowns. We also provide public competitions for several open-world segmentation tasks, spanning from anomaly segmentation to open-world panoptic segmentation.

3 TASK DEFINITIONS

Open-world segmentation tasks are relatively under-explored in the literature, and only recently they are gaining traction thanks to the publication of dedicated benchmarks [6], [10], [58] or the modification of standard closed-world datasets to fit them to the open-world purpose [30], [44]. For this reason, task nomenclature is often ambiguous, and it happens that different previous works name the same task differently. In the following, we attempt to propose an easy-to-understand nomenclature to cover all open-world tasks. A schematic breakdown of the tasks can be found in Fig. 8. Additionally, a visual example is shown in the supplementary material. All tasks that we introduce in the following consider pixel-wise predictions in an image. Moreover, all segmentation

tasks build on top of closed-world segmentation, i.e., they output prediction masks for known classes as well. In the rest of the article, we will refer to these names for everything we address.

3.1 Anomaly Segmentation

SegmentMeIfYouCan [10] was a seminal work in the direction of having segmentation approaches able to deal with unknown objects. They formalize the task of *anomaly segmentation*: given a model trained on a certain number of known categories, the task of anomaly segmentation is the variant of being able to classify an object as belonging to none of them. In this task, there is no concept of unknown class or even object. The input image is simply divided into two separate areas: one belonging to everything that is known (i.e., seen at training time), and another one including everything else.

Given an image $I \in \mathbb{R}^{H \times W}$, the prediction for anomaly segmentation is a mask $M_a \in \{0, 1\}^{H \times W}$, where 0 indicates known and 1 indicates unknown.

3.2 Open-World Semantic Segmentation

Open-world semantic segmentation [75] goes a step beyond anomaly segmentation. Here, the anomalous area is further segmented into different semantic classes. Additionally, these semantic classes stay consistent at test time. For example, let us consider an approach trained on Cityscapes [16]. If, at test time, an image including a pack of zebras and a lion appears, an open-world semantic segmentation approach is able to segment them all as unknown, and to create two new classes, which would correspond to *zebra* and *lion*. Additionally, when a new image containing zebras appear, the approach should be able to assign that area to the already-discovered *zebra* class. This reasoning closely follows standard closed-world semantic segmentation, where areas belonging to the same category across different images are assigned to the same semantic label. Thus, this task has no concept of object instances.

Given an image $I \in \mathbb{R}^{H \times W}$, the prediction for this task is a mask $M_s \in \{0, \dots, K\}^{H \times W}$, where 0 indicates known and $1, \dots, K$ indicate the K categories discovered.

3.3 Open-Set Panoptic Segmentation

The task of open-set panoptic segmentation also extends anomaly segmentation, but is independent from open-world semantic segmentation. This task is more common in the literature [34], [65], and consists of segmenting individual objects within the anomaly segmentation mask. This task does not look at finding new semantic classes, but rather new objects. Following the example mentioned above, if at test time an image containing a pack of zebras and a lion appears, open-set panoptic segmentation segments them all as unknown, and additionally assign a unique instance ID to every individual animal. However, no difference among zebras and lions is made. Generally speaking, this task performs class-agnostic instance segmentation within the anomalous area.

Given an image $I \in \mathbb{R}^{H \times W}$, the prediction for this task is a mask $M_a \in \{0, 1\}^{H \times W}$, where 0 indicates known and 1 indicates unknown, and a mask $M_i \in \{0, \dots, N\}^{H \times W}$ where 0 indicates both known and no object areas, and $1, \dots, N$ indicate the N object instances discovered.

3.4 Open-World Panoptic Segmentation

Open-world panoptic segmentation is a novel task, that builds on open-world semantic segmentation and aims to discover not only novel and consistent semantic classes, but also individual objects within these classes. It goes a step further from open-set panoptic segmentation as well, since the latter does not aim to discover new semantic classes. The task of open-world panoptic segmentation gives a holistic understanding of the scene, since every pixel belongs to a semantic class and will have an instance ID (when applicable), irrespectively of it being *known* or *unknown*.

Given an image $I \in \mathbb{R}^{H \times W}$, the prediction for open-world panoptic segmentation is a mask $M_s \in \{0, \dots, K\}^{H \times W}$, where 0 indicates known and $1, \dots, K$ indicate the K categories discovered, and a mask $M_i \in \{0, \dots, N\}^{H \times W}$, where 0 indicates both known and no object areas, and $1, \dots, N$ indicate the N object instances discovered.

In this article, we propose the first approach and benchmark with a public competition for open-world panoptic segmentation.

4 OUR APPROACH

In this article, we tackle the problem of open-world panoptic segmentation. We propose an approach (see Fig. 4) based on a fully-convolutional neural network with one encoder and three decoders. Our approach builds on top of our previous work ContMAV [75] for open-world semantic segmentation. In the following we explain the details about the whole architecture of Con2MAV, with particular emphasis on what we modified and improved from ContMAV.

4.1 Encoder Architecture

For our task, we use a lightweight fully-convolutional neural network, to facilitate future deployment in the real world. However, our ideas and contributions can be applied to any kind of network. Our CNN is composed of one encoder and three decoders. We use a ResNet34 [29] encoder, where we replaced the standard ResNet block with the NonBottleneck-1D block [68]. This choice is motivated solely from the fact that we aim to make our architecture more lightweight, and the NonBottleneck-1D block replaces all 3×3 convolution by a sequence of 3×1 and 1×3 convolutions with a ReLu in between. Additionally, following the insights from our previous paper [75], we incorporate contextual information by means of a pyramid pooling module [91] at the end of the encoding part.

4.2 Decoder Architectures

Our three decoders have the same structure and are composed of three SwiftNet modules [61] with NonBottleneck-1D blocks, and two final upsampling modules based on nearest-neighbor and depth-wise convolutions [14], that have the major advantage of substantially reducing the computations needed. Following the standard UNet [69] design, we also employ encoder-decoder skip connections after each downsampling stage of the encoder to propagate fine-grained features to the three decoders.

The first decoder, called “semantic decoder”, targets semantic segmentation and additionally tries to build a unique class descriptor for each known category. At inference time, the final features get compared to the known descriptors in order to discriminate between known and unknown classes, which leads to new descriptors. The second decoder, called “contrastive decoder”,

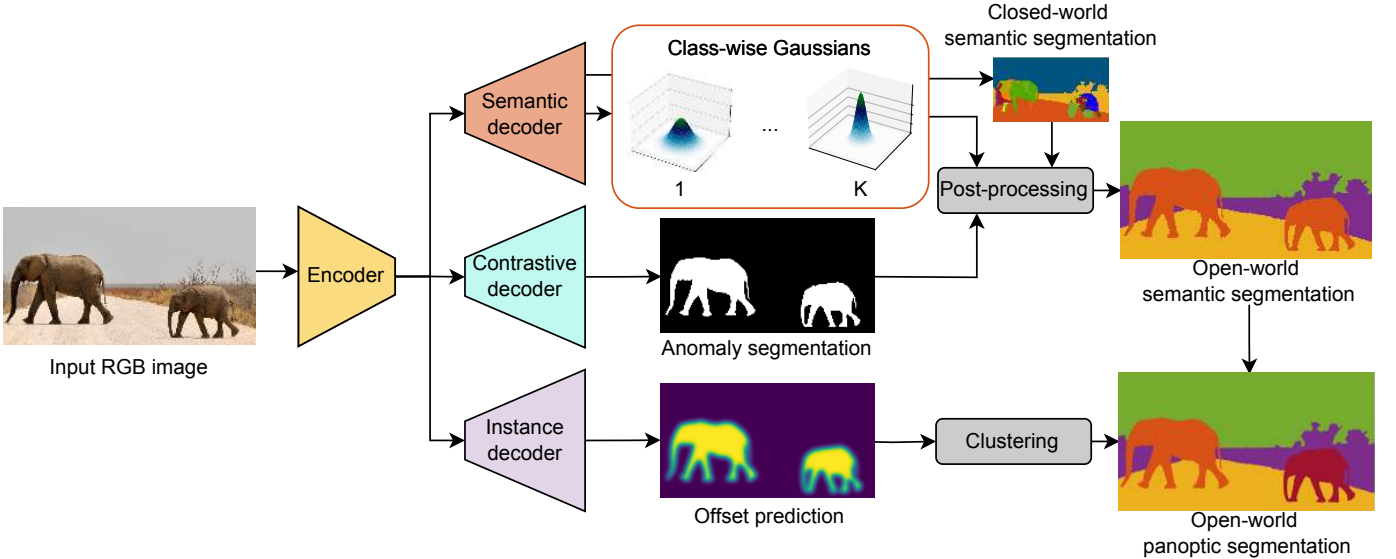


Fig. 4. Our network processes an RGB image via an encoder and three decoders and yields the final open-world panoptic segmentation result.

targets anomaly segmentation and tries to map the features of pixels belonging to known classes on a unit hypersphere, while mapping features of pixels belonging to unknown classes to 0. The third decoder, called “instance decoder”, does not appear in ContMAV and targets class-agnostic instance segmentation by means of vector fields-inspired loss functions [83]. The outputs of the decoder go through different post-processing phases to obtain the final open-world panoptic segmentation result. Further details on the three decoders follow below.

Consider an image $I \in \mathbb{R}^{H \times W}$. In the following, we refer to the set of pixels in the image as $\Omega = \{(1, 1), \dots, (H, W)\}$. Additionally, we call $Y \in \{1, \dots, K\}^{H \times W}$ the ground truth semantic mask of I , where K is the number of known categories used at training time. In contrast, we refer to the predicted (closed-world) semantic mask as $\hat{Y} \in \{1, \dots, K\}^{H \times W}$. Similarly, we call Z the ground truth and \hat{Z} the predicted instance mask, respectively. Finally, we denote with $\Omega_k = \{p \in \Omega \mid Y_p = k\}$ the set of pixels in the image whose ground truth label is k , and with $\hat{\Omega}_k = \{p \in \Omega \mid \hat{Y}_p = Y_p = k\}$ the set of pixels whose predicted label \hat{Y}_p and ground truth label Y_p are both equal to k , i.e., the set of true positives for class k . We do not use bold notation for the pixel tuple p for the sake of clarity.

Semantic Decoder. The semantic decoder aims to perform semantic segmentation and it leverages the standard weighted cross-entropy loss for closed-world semantic segmentation:

$$\mathcal{L}_{\text{sem}} = -\frac{1}{|\Omega|} \sum_{p \in \Omega} \omega_k \mathbf{t}_p^\top \log(\sigma(\mathbf{f}_p)), \quad (1)$$

where ω_k is a class-wise weight computed via the inverse frequency of each class in the dataset, $\mathbf{t} \in \mathbb{R}^{H \times W \times K}$ is the one-hot encoded ground truth annotation of the image, $\mathbf{t}_p \in \mathbb{R}^K$ is the one-hot encoded ground truth annotation at pixel location p , $\sigma(\cdot)$ denotes the softmax operation, and \mathbf{f}_p denotes the pre-softmax feature predicted at pixel p .

Besides the standard closed-world semantic segmentation, our goal with the semantic decoder is also to build a unique class descriptor, or class prototype, for each known class. We already explored this idea in ContMAV [75] and designed a task-specific loss function to deal with this problem. However, this loss function

used pre-softmax features $\mathbf{f}_p \in \mathbb{R}^K$, whose dimension is equal to the number of known classes. When not many classes are available at training time, this class descriptor collapses to a few dimensions, which might be not descriptive enough to reliably discover novel classes. To overcome this problem, we apply this loss function one layer before (intuitively, on the “pre-pre-softmax” features), where the features have a fixed dimension D , that depends on the structure of the network. In the experimental evaluation, we demonstrate how this modification over ContMAV greatly improves performance when dealing with few known categories. In the following, we refer to the features we use for the class descriptor as “pre-logs”, and indicate them with ℓ .

To build the class descriptors, during training we accumulate the pre-logs of all the true positives for each class, where a true positive is a pixel that is correctly segmented. By doing this, we can build a running average class descriptor $\mu_k \in \mathbb{R}^D$ for each class that appears at training time $k \in \{1, \dots, K\}$:

$$\mu_k = \frac{1}{|\hat{\Omega}_k|} \sum_{p \in \hat{\Omega}_k} \ell_p. \quad (2)$$

Together with the mean, we also compute the per-class variance $\sigma_k^2 \in \mathbb{R}^D$ via the sum of squares:

$$\sigma_k^2 = \frac{1}{|\hat{\Omega}_k|} \sum_{p \in \hat{\Omega}_k} (\ell_p - \mu_k) \odot (\ell_p - \mu_k), \quad (3)$$

where \odot indicates the element-wise product (Hadamard product).

At the beginning of epoch e , each category has a mean and a variance μ_k^{e-1} and σ_k^{e-1} , computed at the previous epoch $e-1$. The goal of having a unique class descriptor for each known class is that the prediction at each pixel belonging to that class must be equal to the descriptor. Thus, we use the feature loss function $\mathcal{L}_{\text{feat}}$ at the pre-logit level given by

$$\mathcal{L}_{\text{feat}} = \frac{1}{|\Omega|} \sum_{k=1}^K \sum_{p \in \Omega_k} \frac{\|\ell_p - \mu_k^{e-1}\|^2}{(\sigma_k^{e-1})^2}. \quad (4)$$

The overall idea is that the true positives for each class contribute to building the class descriptor in Eq. (2), which is then

used for optimization in the next epoch for all pixels belonging to each class. For this reason, this loss function is not active during the very first epoch of the training phase, which is used to start building the descriptor. The class descriptors are learned during training and constantly optimized, based on the predictions of each epoch.

The semantic decoder is optimized with a weighted sum of the loss functions introduced above:

$$\mathcal{L}_{\text{sdec}} = w_1 \mathcal{L}_{\text{sem}} + w_2 \mathcal{L}_{\text{feat}}. \quad (5)$$

Contrastive Decoder. The contrastive decoder also operates at the pre-logit level and tackles anomaly segmentation by combining the contrastive loss [11] and the objectsphere loss [19]. To do so, we first compute the mean pre-logit $\bar{\ell}_k \in \mathbb{R}^D$ for each class k in the current image

$$\bar{\ell}_k = \frac{1}{|\Omega_k|} \sum_{p \in \Omega_k} \ell_p. \quad (6)$$

Notice that we are again using the pre-logit as in the semantic decoder. The pre-logit feature $\ell_p \in \mathbb{R}^D$ used here is obviously different from the previous one, since it comes from a different decoder. We compute the contrastive loss $\mathcal{L}_{\text{cont}}$ such that $\bar{\ell}_k$ approximates the normalized mean representation $\bar{\mu}_k^{e-1}$ of the corresponding class in the previous epoch μ_k^{e-1} and gets dissimilar from the other classes mean representation:

$$\mathcal{L}_{\text{cont}} = - \sum_{k=1}^K \log \frac{\exp(\bar{\ell}_k^\top \bar{\mu}_k^{e-1} / \tau)}{\sum_{i=1}^K \exp(\bar{\ell}_k^\top \bar{\mu}_i^{e-1} / \tau)}, \quad (7)$$

where τ is a temperature parameter. The goal of this loss function is to have $\bar{\ell}_k$ approximate the corresponding vector in the feature bank, i.e., the normalized class descriptors $\bar{\mu}_k^{e-1}$. To achieve this, we changed from the pre-softmax features to the pre-logit in this loss function, in order to have dimensionally-consistent vectors. The outcome of the contrastive loss is to scatter the class-specific pre-logits on the unit hypersphere. Additionally, we use the objectsphere loss function

$$\mathcal{L}_{\text{obj}} = \begin{cases} \max(1 - \|\ell_p\|^2, 0) & , \text{if } p \in \Omega_k \\ \|\ell_p\|^2 & , \text{otherwise} \end{cases}, \quad (8)$$

where Ω_k is the set of pixels in the image belonging to known classes. The other pixels at training time include only the void (i.e., unlabeled) areas of the image. This loss function aims to make the norm of the pre-logit of known classes larger than 1, and the norm of the pre-logit of unknown classes equal to 0. We could have used any other value instead of 1 in principle, but since we are combining contrastive and objectsphere loss, this would not be meaningful. The contrastive loss in Eq. (7) aims to distribute all feature vectors on the unit sphere, due to the use of normalized vectors in the feature bank. Thus, any value in the objectsphere loss different than 1 would reduce the synergy between the two losses. Especially using a value larger than 1 means that the two losses would try to achieve incompatible tasks, i.e., making the norm of the features larger than 1 while simultaneously pushing them to lie on the unit sphere.

We show a 2D depiction of the interaction between these two loss functions in the supplementary material along with some more considerations about their synergy.

We optimize the contrastive decoder with a weighted sum of the loss functions introduced above, resulting in:

$$\mathcal{L}_{\text{cdec}} = w_3 \mathcal{L}_{\text{cont}} + w_4 \mathcal{L}_{\text{obj}}. \quad (9)$$

Instance Decoder. The instance decoder addresses class-agnostic instance segmentation, where we predict a 2D offset for each pixel, so that pixels belonging to the same object instance point to the same area in the image and can be clustered together.

Given an instance $\mathcal{C}_j \in \Omega$, defined as the set of pixels of the images belonging to the j -th object instance, with a centroid \mathbf{c}_j , we want to obtain offset vectors for all pixels belonging to \mathcal{C}_j that point toward \mathbf{c}_j , while the remaining offset vectors should not. We achieve this by means of the Lovász Hinge loss [59]

$$\mathcal{L}_{\text{off}} = \frac{1}{|\mathcal{C}|} \sum_{j=1}^{|\mathcal{C}|} \text{Lovász}(\mathbf{F}_{\mathcal{C}_j}, \mathbf{G}_{\mathcal{C}_j}). \quad (10)$$

In this equation, $\mathbf{F}_{\mathcal{C}_j} \in \mathbb{R}^{H \times W}$ is a soft-mask obtained by the offset predictions, while $\mathbf{G}_{\mathcal{C}_j} \in \{0, 1\}^{H \times W}$ denotes the binary ground truth mask of the j -th instances. The soft mask $\mathbf{F}_{\mathcal{C}_j}$ for instance \mathcal{C}_j is obtained from the offset prediction: each pixel gets a score that depends on how far from the instance centroid its offset points to. This is formalized as

$$f_{\mathcal{C}_j} = \exp\left(-\frac{\|e_p - \mathbf{c}_j\|^2}{2\eta^2}\right), \quad (11)$$

where $e_p = p$ indicates the pixel location pointed by the prediction at pixel p , and η is a hyperparameter that defines an isotropic clustering region around the centroid.

This loss function encourages the network to predict, for all pixels associated with a specific instance, an offset vector that points toward their corresponding centroid. Simultaneously, it penalizes offset vectors that point towards a different centroid than their own. In this way, the offsets of different instances form clusters in the 2D space. Note that it is not necessary for a centroid to be inside the instance for having instance-wise clusters.

Inspired by the work by Weyler et al. [83], we use the divergence and curl loss functions to strengthen our offset predictions. These two loss functions are inspired by the concept of vector field in physics. Imagine the vector field as a fluid flow. A positive vector field divergence indicates a source from which all particles flow away. In contrast, a negative divergence indicates a sink to which all particles are flowing. This translates well to the instance segmentation case as we want all pixels belonging to a certain instance to point toward their respective centroid. The curl, instead, indicates a rotational behavior in the vector field. Specifically, a positive curl indicates a counter-clockwise rotation, while a negative curl implies a clockwise rotation.

Following Weyler et al. [83], for formalizing the divergence and curl loss functions, we need a simplified vector field defined by a continuous multivariable function $\mathbf{O}(h, w) : \mathbb{R}^2 \rightarrow \mathbb{R}^2$

$$\mathbf{O}(h, w) = \begin{bmatrix} o_h(h, w) \\ o_w(h, w) \end{bmatrix} = \begin{bmatrix} -h + c_h \\ -w + c_w \end{bmatrix}, \quad (12)$$

that behaves as a perfect sink, i.e., all offset vectors point toward $\mathbf{c} = [c_h, c_w]^\top$. In 2D, divergence is defined as

$$\text{div } \mathbf{O} := \frac{\partial o_h(h, w)}{\partial h} + \frac{\partial o_w(h, w)}{\partial w}. \quad (13)$$

Thus $\frac{\partial o_h(h, w)}{\partial h} = \frac{\partial o_w(h, w)}{\partial w} = -1$ and $\text{div } \mathbf{O} = -2$. The divergence should then be equal to -2 , and additionally its two components must be equal. This is achieved by two regression

loss functions:

$$\begin{aligned}\mathcal{L}_{\text{div}} &= \frac{1}{|\Omega|} \sum_{p \in \Omega} \rho \left((\text{div } \mathbf{O})_p - (-2) \right) \\ \mathcal{L}_{\text{div}}^{\text{aux}} &= \frac{1}{|\Omega|} \sum_{(h,w) \in \Omega} \rho \left(\frac{\partial o_h(h,w)}{\partial h} - \frac{\partial o_w(h,w)}{\partial w} \right),\end{aligned}\quad (14)$$

where $\rho(\cdot)$ denotes the Geman-McClure loss [2], and (h, w) denote the image coordinates of pixel p .

The curl is defined as

$$\text{curl } \mathbf{O} := \frac{\partial o_h(h,w)}{\partial w} - \frac{\partial o_w(h,w)}{\partial h}.\quad (15)$$

When applying the curl to the vector field in Eq. (12), we obtain $\frac{\partial o_h(h,w)}{\partial w} = \frac{\partial o_w(h,w)}{\partial h} = 0$, which imply $\text{curl } \mathbf{O} = 0$. Concretely speaking, this means we want no rotational behavior in our vector field. We formalize two loss functions to have the curl equal to zero and the two partial derivatives to be equal to each other:

$$\begin{aligned}\mathcal{L}_{\text{curl}} &= \frac{1}{|\Omega|} \sum_{p \in \Omega} \rho \left((\text{curl } \mathbf{O})_p \right) \\ \mathcal{L}_{\text{curl}}^{\text{aux}} &= \frac{1}{|\Omega|} \sum_{(h,w) \in \Omega} \rho \left(\frac{\partial o_h(h,w)}{\partial w} - \frac{\partial o_w(h,w)}{\partial h} \right).\end{aligned}\quad (16)$$

For further details, we refer to the work by Weyler et al. [83]. Finally, the instance decoder is optimized with the weighted sum of the loss functions introduced so far

$$\begin{aligned}\mathcal{L}_{\text{ins}} &= w_5 \mathcal{L}_{\text{off}} + w_6 \mathcal{L}_{\text{div}} + w_7 \mathcal{L}_{\text{div}}^{\text{aux}} + \\ &w_8 \mathcal{L}_{\text{curl}} + w_9 \mathcal{L}_{\text{curl}}^{\text{aux}}.\end{aligned}\quad (17)$$

4.3 Post-Processing

Post-Processing for Anomaly Segmentation. We obtain anomaly segmentation results by fusing the outputs of the semantic and contrastive decoders. The semantic decoder yields closed-world semantic segmentation, but simultaneously builds individual class descriptors in the pre-logit space for each known class. Thanks to the mean $\boldsymbol{\mu}_k \in \mathbb{R}^D$ and variance $\boldsymbol{\sigma}_k^2 \in \mathbb{R}^D$, that we built for each known class $k = 1, \dots, K$, we can construct a multi-variate normal distribution $\mathcal{N}_k(\boldsymbol{\mu}_k, \boldsymbol{\Sigma}_k)$, where $\boldsymbol{\Sigma}_k = \text{diag}(\boldsymbol{\sigma}_k^2)$ is the covariance matrix, which we obtain from the variance assuming that all classes are independent. In this way, when we predicted a pre-logit ℓ_p at pixel p , we can compute its fitting score to each known category by means of the squared exponential kernel

$$s_k(\ell_p) = \exp \left(-\frac{1}{2} (\ell_p - \boldsymbol{\mu}_k)^\top \boldsymbol{\Sigma}_k^{-1} (\ell_p - \boldsymbol{\mu}_k) \right).\quad (18)$$

Then, we take the highest score

$$s(p) = \max_k s_k(\ell_p),\quad (19)$$

which would correspond to the closest known category to the predicted pixel. Notice that, at test time, this process overrides the standard procedure for closed-world semantic segmentation, which consists in taking the pre-softmax feature and applying an $\text{argmax}(\cdot)$ operator to find which class the pixel belongs to. Once we get the score $s(p)$, we need a strategy that discriminates among known, i.e., the pixel belongs to the class k that maximizes Eq. (19), or unknown. Remember that, by means of the feature loss function in Eq. (4), the pre-logit of pixels belonging to a class are optimized to be as close as possible to the descriptor. For this reason, we use a simple 1σ bound as a

decision mechanism. In this way, we have with $s_{\text{unk},p}^{\text{sem}} \in \{0, 1\}$, a boolean variable indicating whether the pixel is unknown or not.

The contrastive decoder aims to have all features of pixels belonging to known classes with norm close to 1, and features of pixels belonging to unknown classes with norm close to 0. We assume that samples corresponding to unknown are distributed as a normal around 0. In this scenario, all samples corresponding to known classes, which should fall on the unit circle, are outliers. Thus we expect our unknown samples to be distributed as $\mathcal{N}(0, 1)$. We use the 1σ bound to get $s_{\text{unk},p}^{\text{con}} \in \{0, 1\}$, a boolean variable indicating whether the pixel is unknown or not.

Finally, we consider a pixel to be unknown only if both $s_{\text{unk},p}^{\text{sem}} = 1$ and $s_{\text{unk},p}^{\text{con}} = 1$.

Post-Processing for Open-World Semantic Segmentation.

At test time, we have K pre-logit descriptors ℓ_k , where K indicates the number of known categories. For each pixel, we predict the closest category to it indicated by the outcome of Eq. (19). As described in the open-world semantic segmentation task, we want our discovered classes to be consistent in the dataset. This means that if an anomalous area of the same category of p appears in a future image, we want to be able to put them together. Thus, the first time an anomalous pixel appears, we save the descriptor $\ell_p \in \mathbb{R}^D$ together with all others, which leads to having an additional known class $K \leftarrow K+1$. Basically, we treat our newly-discovered category as a “new known” class. Our database of descriptors is composed by \bar{K} , where $\bar{K} = K + K_{\text{unk}}$ and K_{unk} is the number of unknown classes discovered so far. It is important to notice that we allow the K_{unk} pre-logit descriptors of the “new known” classes to evolve. The K descriptors of the known classes are accumulated during training, and thus they are not allowed to change at test time. However, we obviously do not have any descriptor for the unknown classes at the end of the training. The first time we discover a novel class, we save its descriptor and then follow the same procedure used at training time to build the mean descriptor of the class using a running average and running variance. The main difference is that at training time, we have access to the ground truth annotation, and therefore we only use the true positives to do that, see Eq. (2), while at test time we consider all pre-logits predicted as a certain class.

Post-Processing for Open-World Panoptic Segmentation.

The instance decoder yields offset predictions, where pixels belonging to the same instance point to the same area, while pixels belonging to different instances point to different areas. We use HDBScan [51] to cluster the offset predictions. We execute the clustering only in the “thing” areas, which means all the known classes that are known to have instances, and all the unknown categories. The result is then filtered by the semantic prediction in order to enforce consistency. This last step is necessary in order to disallow pixels from different semantic classes to mistakenly being grouped into the same instance. Roughly speaking, we decide to “trust” the semantic prediction more than the instance.

5 PANIC DATASET

In this article, we provide a new valuable dataset called PANIC (Panoptic Anomalies In Context), an open-world panoptic segmentation test set in the autonomous driving context. Datasets for anomaly and open-world segmentation are rare compared to closed-world segmentation ones. PANIC is composed of 800 images, and contains 58 unknown categories. Similarly to Segment-MeIfYouCan [10], we consider Cityscapes [16] as the standard

Dataset	Images		Semantic Classes	Instances	Hidden Test Set
	Val	Test			
Fishyscapes Lost-and-Found [6]	373	1203	N.A.	1864	✓
CAOS BDDAnomaly [30]	0	810	3	1231	✗
RoadObstacle21 [10]	0	327	N.A.	388	✓
SegmentMeIfYouCan [10]	10	100	N.A.	262	✓
PANIC (ours)	131	679	58	4029	✓

TABLE 1. Main properties of open-world segmentation datasets. In the semantic classes, “N.A.” means that semantic labels are not available. For example, SegmentMeIfYouCan, despite having 26 different types of anomalous objects, does not provide any semantic annotations.

training set with known classes. The 58 categories are split into two groups: validation classes and test classes. Validation categories are either less interesting classes, or classes that appear in Cityscapes in the void area (i.e., unlabeled). Such classes are, for example, garbage bins, parkimeters, monuments, etc. Test classes are, instead, more challenging objects such as electric scooters, recumbent bicycles, forklifts, etc. Thus, we split the dataset in two parts: the validation set, containing only validation classes, and the test set, containing both validation and test classes. Following the nomenclature introduced by Bendale et al. [4], our validation set contains only the so-called *known unknown*, i.e., those classes that do not have a label to optimize for during training, but still appear at training time in the void/unlabeled area. The test set, instead, contains also *unknown unknowns*, i.e., categories that are completely absent from the training set. We release image and ground truths for the validation set, and images only for the hidden test set which is used for the competitions mentioned below.

A comparison among previously-published datasets and our dataset can be found in Tab. 1. LostAndFound [6] contains 9 different types of anomalies, but it considers children and bicycles as anomalies, even though they are part of the Cityscapes training set. The CAOS BDD-Anomaly benchmark [30] suffers from a similar low-diversity issue, since it samples from the BDD100K dataset [88] to build a test set containing only 3 object classes. Both, Fishyscapes and CAOS, try to mitigate this low diversity by introducing synthetic data in the dataset. Synthetic data, however, is not realistic and not representative of the situations that can arise in real world scenarios. RoadObstacle21 and SegmentMeIfYouCan (also known as RoadAnomaly21 in the original paper) [10], instead, despite proposing a dataset containing multiple kinds of objects, only focus on anomaly segmentation, without providing annotations and evaluation for discovering new classes and individual objects. Recently, Nekrasov et al. [58] provided instance-level annotation for SegmentMeIfYouCan, RoadObstacle21, and Fishyscapes, but do not provide semantic annotations. Their work falls into the category that we called open-set panoptic segmentation, yielding an anomaly mask with object instances, without differentiating among objects belonging to different categories.

In PANIC, anomalies can appear anywhere in the image. They can have any size, and are not limited to active traffic participants. We provide pixel-wise annotations of semantic classes and individual object instances.

5.1 Data Collection and Labeling

We recorded all images of PANIC in Bonn, Germany, with our instrumental car, using the sensor platform described by Vizzo et al. [79]. We recorded with two different settings. The most common case is with the sensor platform mounted on top of our car. A small subset of images is instead recorded with the sensor platform mounted on a manually-pushed vehicle. Thus, there are two different point of views for the images. We only took images

recorded with the front camera of the sensor platform. The camera is a Basler Ace acA2040-35gc. After recording, we sampled a subset of the recorded images in order to avoid duplicates and filter out images that did not contain any anomalous object, and labeled them using the online tool segments.ai. The 19 Cityscapes evaluation classes [16] on which most segmentation models for autonomous driving are trained, serve as basis to determine anomalies. Everything that belongs to any of those 19 classes is labeled as “not anomaly”. For all the rest, we provide a pixel-wise semantic and instance annotation. To comply with privacy restrictions, we anonymize all faces, license plates, and windows of private buildings when necessary. The images we provide have those areas in black. This does not bias any learning algorithm, since the dataset we propose is supposed to be an evaluation-only dataset, and the training happens on Cityscapes, which provides the known classes. Additionally, we label an “ignore” class that will not be included in the evaluation, that covers the egovehicle and the anonymized areas.

5.2 Benchmarks and Metrics

We propose four benchmarks accompanied by public Codabench competitions [87], one for each of the segmentation tasks described in Sec. 3. Each has its own evaluation pipeline and metrics.

5.2.1 Anomaly Segmentation

Following the insights from SegmentMeIfYouCan [10], we propose two groups of metrics for evaluating anomaly segmentation: pixel-level metrics and component-level metrics.

The first pixel-level metric is the area under the precision-recall curve (AUPR) that evaluates the separability of the pixel-wise anomaly scores between known and unknown, putting more emphasis on the minority class. This makes it generally good for anomaly segmentation, since often the anomalies are less prominent than the known classes in the image. The other pixel-level metric is the false positive rate at 95% true positive rate (FPR95), that indicates how many false positive predictions must be made to reach the desired true positive rate (i.e., 95%).

Pixel-level metrics, however, fail to properly evaluate small anomalies. Component-level metrics are better in evaluating all anomalous regions in the scene, irrespectively of their size. SegmentMeIfYouCan [10] introduces three metrics for component-level evaluation: the segment-wise intersection over union (sIoU) for evaluating true positive and false negatives, the positive predicted value (PPV, or component-wise precision) for taking into account false positives, and the component-wise F1-score which summarizes true positive, false positive, and false negative. For further details, insights, and considerations on anomaly segmentation metrics, we refer to the original paper [10].

We decided to not use the area under the ROC curve (AUROC), because recently several papers showed its limitations [27], [33], [82], as two models with the same performance may differ

Dataset	Modality	mIoU [%] \uparrow	PQ [%] \uparrow
Cityscapes	CW	71.1	-
	OW	68.3	-
COCO	CW	71.9	43.8
	OW (K = 5%)	70.0	43.6
	OW (K = 10%)	68.5	39.8
	OW (K = 20%)	65.6	39.1
BDDAnomaly	CW	64.6	-
	OW	62.4	-
SUIM	CW	68.6	-
	OW	60.0	-

TABLE 2. Results comparison between our model trained in a closed- and open-world fashion on the different datasets we use. Metrics are computed only on known classes, to show that the open-world modality does not significantly harm closed-world performances.

substantially in terms of how clearly they separate in-distribution and out-of-distribution samples. In general, these works argue that AUROC is not a fair metric for comparing different approaches.

5.2.2 Open-World Semantic Segmentation

The task of open-world semantic segmentation is not common in the literature, thus a proper evaluation pipeline does not exist. Since standard semantic segmentation is comprehensively evaluated via the intersection over union (IoU) [20], we aim to expand the concept of intersection over union to the open-world case.

The closed-world IoU is typically computed by building a confusion matrix $C \in \mathbb{R}^{K \times K}$, with K the number of known classes, in which the i -th row indicates, for each class, how many pixels have been predicted as belonging to category i . In this case, predicted class i refers to ground truth class i . A perfect IoU of 1.0 is obtained when entry (ii) of the confusion matrix is equal to the number of pixels belonging to ground truth class i , and both the i -th row and i -th column have no entry different from 0 but the i -th one. In the following, we indicate as $\text{row}_i \in \mathbb{R}^K$ the i -th row of a confusion matrix. Similarly, $\text{column}_k \in \mathbb{R}^K$ is the k -th column of the confusion matrix. The closed-world IoU concept can easily be extended to the open-world case, with two major modifications:

- 1) The open-world confusion matrix should not be square, as it is possible that the evaluated approach discovers a different number of categories \tilde{K} than the ones that are actually annotated. The confusion matrix will have dimension $\tilde{K} \times K$, where the number of rows \tilde{K} refers to the newly-discovered classes, and the number of columns K is fixed and corresponds to the ground truth classes.
- 2) In the open-world IoU computation, the predicted class corresponding to row i of the confusion matrix does not have to be matched to ground truth class i , but rather to $\text{argmax}(\text{row}_i)$, where $\text{row}_i \in \mathbb{R}^K$ and $i \in \{1, \dots, \tilde{K}\}$. Simply put, in open-world semantic segmentation, we do not expect a precise mapping in which predicted class i corresponds to ground truth class i , but we allow predicted class i to match to ground truth class j . This is possible because, as we do not explicitly optimize for categories, we have no control over the order in which we discover new classes.

Beside the open-world IoU, we are also interested in understanding how reliable our predictions are. To this end, we report two clustering metrics that are particularly fitting for our case,

namely homogeneity and completeness [70]. Homogeneity is a measure of the ratio of samples of a single class pertaining to a single cluster. The fewer different classes included in one cluster, the better. In our case, the clusters are the predicted categories, and homogeneity Hom_i measures how consistent is a certain predicted label, i.e., how closely follow a certain ground truth class or is spread among multiple ones. It is computed as

$$\text{Hom}_i = \frac{\max(\text{row}_i)}{\sum \text{row}_i}, \quad \forall i \in \{1, \dots, \tilde{K}\}. \quad (20)$$

Conversely, completeness Com_k measures the ratio of pixels of a given class that is assigned to the same cluster. In our case, it measures how consistently a certain ground truth category is predicted, i.e., if it is regularly predicted as the same class or if it is spread among many predicted classes. It is computed as

$$\text{Com}_k = \frac{\max(\text{column}_k)}{\sum \text{column}_k}, \quad \forall k \in \{1, \dots, K\}. \quad (21)$$

5.2.3 Open-Set Panoptic Segmentation

Open-set panoptic segmentation is evaluated by means of the panoptic quality [39]. This evaluation procedure has been adopted by previous approaches [65], and we follow it here. In this case, there are no semantic classes but only two categories, known and unknown. The unknown area contains object instances, while the known area is treated as “stuff”, so that the quality of the closed-world instance segmentation does not affect the final panoptic quality. We also report segmentation and recognition quality.

5.2.4 Open-World Panoptic Segmentation

Since there is no prior work on open-world panoptic segmentation, we decide to evaluate it in a way that is as close as possible to standard closed-world panoptic segmentation. We report open-world mean intersection over union, panoptic quality, recognition quality, and segmentation quality. Differently from open-set panoptic segmentation, in this case the panoptic quality evaluates multiple unknown categories, split among *things* and *stuff*. We also report completeness and homogeneity.

6 EXPERIMENTAL EVALUATION

The main focus of this work is an approach for open-world panoptic segmentation. We present extensive experiments on multiple datasets to show the capabilities of our method. The results of our experiments show that our model achieves state-of-the-art results for all open-world tasks described in Sec. 3, while performing competitively on the known classes. Additionally, we show how our new dataset, PANIC, enables all kind of open-world task while being extremely challenging.

6.1 Experimental Setup

We use multiple datasets for validating our method. For anomaly segmentation, we use SegmentMeIfYouCan [10] and submit our prediction to the public challenge, BDDAnomaly, and our proposed dataset PANIC. For open-world semantic segmentation, we use BDDAnomaly [30], COCO [44], SUIM [35], and PANIC. BDDAnomaly samples from BDD100K and removes all images containing bicycles, motorcycles, and trains from the training set, to create an open-world test set. Similarly, Mask2Anomaly [65] proposes three open-world splits of COCO, in which 5%, 10%, and 20% of ground truth categories are discarded from the training

Approach	OoD	Pixel-Level		Component-Level		
		AUPR [%] ↑	FPR95 [%] ↓	sIoU gt [%] ↑	PPV [%] ↑	mean F1 [%] ↑
DenseHybrid [25]	✓	78.0	9.8	54.2	24.1	31.1
RbA [56]	✓	94.5	4.6	64.9	47.5	51.9
UNO [17]	✓	96.3	2.0	68.5	55.8	62.6
Maskomaly [1]	✗	93.4	6.9	55.4	51.2	49.9
RbA [56]	✗	86.1	15.9	56.3	41.4	42.0
ContMAV [75]	✗	90.2	3.8	54.5	61.9	63.6
UNO [17]	✗	96.1	2.3	68.0	51.9	58.9
Con2MAV (ours)	✗	90.0	2.7	59.1	68.3	69.4

TABLE 3. Anomaly segmentation results on the SegmentMeIfYouCan test set. We separate methods that use external data, i.e. out of distribution (OoD) data with semantic labels different from the ones in Cityscapes, during training. Best results are highlighted in bold. For more results, check the public leaderboard at <https://segmentmeifyoucan.com/leaderboard>.

Approach	Pixel-Level		Component-Level		
	AUPR [%] ↑	FPR95 [%] ↓	sIoU gt [%] ↑	PPV [%] ↑	mean F1 [%] ↑
ContMAV [75]	91.7	66.4	15.0	72.1	24.2
Con2MAV (ours)	95.7	35.3	20.9	64.7	31.2

TABLE 4. Anomaly segmentation results on the hidden test set of our dataset, PANIC. Best results are highlighted in bold. Public competition is available at <https://www.codabench.org/competitions/4561>.

set to create an open-world test set, respectively. We did the same for the underwater dataset SUIM, and discarded all images containing annotations of humans, robots, and wrecks & ruins. For open-set panoptic segmentation, we use COCO and PANIC. Finally, for open-world panoptic segmentation, we use PANIC.

Training details and parameters. In all experiments, we use the one-cycle learning rate policy [73] with an initial learning rate of 0.004. We perform random scale, crop, and flip data augmentations, and optimize with Adam [37] for 200 epochs with batch size 16. We set loss weights $w_1 = 0.8$, $w_2 = 0.2$, $w_3 = 0.5$, $w_4 = 0.5$, $w_5 = 0.4$, $w_6 = 0.2$, $w_7 = 0.1$, $w_8 = 0.2$, and $w_9 = 0.1$. We set $\tau = 0.1$, as proposed by Chen et al. [11]. For SegmentMeIfYouCan and PANIC, we train only on Cityscapes. For BDDAnomaly, COCO, and SUIM, we train only on their own training sets.

6.2 Closed-World Performance

Our approach, while providing state-of-the-art open-world predictions, also yields compelling closed-world performance. In particular, the performance of our approach on the closed-world categories is not harmed by the open-world nature of the CNN. In Tab. 2, we show the performance of our method in terms of mIoU and PQ on all datasets on the known categories only. In the table, “OW” stands for the approach we describe in Sec. 4, while “CW” stands for the same approach with all the open-world components (i.e., feature loss function and contrastive decoder) removed. The table shows that our open-world design does not significantly harm segmentation performance on the known classes.

6.3 Anomaly Segmentation

This set of experiments shows that our approach achieves state-of-the-art results on anomaly segmentation. We report results on SegmentMeIfYouCan in Tab. 3, PANIC in Tab. 16, and BDDAnomaly in Tab. 5. We achieve compelling results on all three datasets, consistently outperforming the baselines. Additionally, we outperform our previous approach ContMAV on all datasets. While the difference is less evident on SegmentMeIfYouCan and BDDAnomaly,

Approach	AUPR [%] ↑	FPR95 [%] ↓
MaxSoftmax [31]	3.7	24.5
Background [7]	1.1	40.1
MC Dropout [21]	4.3	16.6
Confidence [18]	3.9	24.5
MaxLogit [30]	5.4	14.0
ContMAV [75]	96.1	6.9
Con2MAV (ours)	97.9	5.8

TABLE 5. Anomaly segmentation results on BDDAnomaly. Best results are highlighted in bold.

mostly due to the fact that ContMAV already performed quite competitively, results on PANIC show how Con2MAV is substantially more reliable when dealing with a challenging dataset, outperforming ContMAV by several percentage points on four out of five metrics. Additionally, on SegmentMeIfYouCan we rank top 1 in two component-level metrics, outperforming also approaches that use out-of-distribution data for the training.

By looking at the performance of both ContMAV and Con2MAV, we can also see how PANIC is a very challenging dataset even for a simple task such as anomaly segmentation. In fact, both approaches suffer a heavy drop in performance when compared to SegmentMeIfYouCan. Both ContMAV and Con2MAV achieve good performance on PANIC on AUPR and PPV. Intuitively, AUPR is high when there is a sharp difference in the probability heatmap between unknown and known areas, while PPV is high when there are few false positive predictions. High scores mean that both ContMAV and Con2MAV act quite conservatively on PANIC, being very confident in the prediction of anomalous areas, despite having false negatives. This is a further measure of how challenging our dataset is compared to others.

6.4 Open-World Semantic Segmentation

The second set of experiments is about open-world semantic segmentation. This task is enabled by the feature loss reported in Eq. (4). Since the task is uncommon in literature, we compare against our previous approach, ContMAV [75]. As in our

K %	Approach	mIoU [%] ↑
5	Background + cluster	8.4
	ContMAV (no feat loss) [75]	23.5
	ContMAV (with feat loss) [75]	40.0
	Con2MAV (ours)	50.5
10	Background + cluster	6.1
	ContMAV (no feat loss) [75]	18.8
	ContMAV (with feat loss) [75]	38.5
	Con2MAV (ours)	48.5
20	Background + cluster	1.2
	ContMAV (no feat loss) [75]	15.0
	ContMAV (with feat loss) [75]	33.4
	Con2MAV (ours)	48.5

TABLE 6. Open-world semantic segmentation results on the COCO validation set on three different known-unknown splits. K denotes the percentage of unknown classes present in the dataset. Best results are highlighted in bold.

Approach	IoU [%] ↑			mIoU [%] ↑
	Train	Motorcycle	Bicycle	
Background + cluster	0	32.3	32.8	21.7
ContMAV [75]	62.4	62.2	56.8	60.5
Con2MAV (ours)	66.5	64.4	53.8	61.6
Closed-world	72.3	69.3	60.9	67.5

TABLE 7. Open-world semantic segmentation results on BDDAnomaly. Best results are highlighted in bold.

previous paper, we report one baseline as lower bound, that uses the background class for the unknowns and performs K-means clustering in the feature space for this class to extract unknown classes. We report results on COCO in Tab. 6, BDDAnomaly in Tab. 7, and PANIC in Tab. 17. On COCO, we consistently outperform ContMAV by at least 10% in the mIoU computation. On BDDAnomaly, we outperform ContMAV in two out of three unknown classes, while getting close to the performance of the closed-world model, reported as a performance upper bound. On PANIC, we improve ContMAV by almost 5% mIoU, despite our previous approach achieves a better completeness.

In Tab. 9, we also compare ContMAV and our current approach Con2MAV on the underwater dataset SUIM [35]. SUIM has only 7 semantic classes, and we discarded 3 from the training and validation set in order to create an open-world test set, similarly to what it has been done for BDDAnomaly and COCO. We use this dataset because we want to test how Con2MAV compares to ContMAV when only few known training classes are available, which is one of the main limitations of our previous work. Thus, we reduce the number of training classes to just 4. Our goal is to validate our design choice of building the class descriptor at pre-logit level, rather than at pre-softmax level as we did in ContMAV. As discussed, this design decision is explicitly motivated by the fact that our previous approach did not perform well when the training classes are few. The results show that our design choice successfully addressed this issue, as we outperform ContMAV by 19% mIoU, and up to 28% in a single individual category (namely, “wreck & ruins”). We show qualitative results in Fig. 5.

6.5 Open-Set Panoptic Segmentation

Our third set of experiments is about open-set panoptic segmentation. For this task, we use COCO and PANIC. In COCO, we compare with other approaches that dealt with this task, and report

Approach	Unknown Classes		
	mIoU [%] ↑	Com [%] ↑	Hom [%] ↑
ContMAV [75]	15.8	81.4	77.3
Con2MAV (ours)	20.2	77.6	78.3

TABLE 8. Open-world semantic segmentation results on the hidden test set of our dataset, PANIC. “Com” and “Hom” stand for completeness and homogeneity, respectively. Best results are highlighted in bold. Public competition is available at <https://www.codabench.org/competitions/4563>.

Approach	IoU [%] ↑			mIoU [%] ↑
	Human	Wrecks & Ruins	Robot	
ContMAV [75]	46.2	36.9	46.2	43.1
Con2MAV (ours)	69.4	64.3	53.0	62.2
Closed-world	82.0	71.6	80.2	77.9

TABLE 9. Open-world semantic segmentation results on the SUIM dataset. Best results are highlighted in bold.

results in Tab. 10. We consistently outperform all baselines in all metrics. Additionally, while the baselines drop in performance when increasing the open-world set dimension (i.e., when K grows), our performance remains similar. We show qualitative results in Fig. 6. We report results on PANIC in Tab. 18. It is interesting to note that our performance on PANIC is quite similar to what we achieve on COCO, especially in the more challenging splits (10% and 20%). This is a further indication of how challenging our dataset is.

6.6 Open-World Panoptic Segmentation

The last experiment shows our performance on open-world panoptic segmentation on PANIC. The results are reported in Tab. 15. For this novel variant of open-world perception there is no baseline to compare to. Our approach still achieves a satisfactory 24.3% panoptic quality, and especially has good performance when it comes to completeness and homogeneity. This means that the categories we predict do not span over multiple ground truth classes but stay close to a single one, and that our ground truth categories are not predicted as many categories at once, but the prediction is quite consistent. We show qualitative results in Fig. 7.

6.7 Ablation Studies

Finally, we provide ablation studies to investigate the individual contribution of the modules we introduced. We perform all ablation studies on BDDAnomaly since we have access to test set ground truth labels. Additionally, we used BDDAnomaly also for the ablation studies in our previous paper [75], so we do the same here in order to facilitate the comparison.

The first ablation study shows the contribution of using the pre-logit instead of the pre-softmax features for computing the loss functions of the semantic and contrastive decoder, and the impact of having auto-tuned thresholds in the post-processing mechanisms. The approach without both pre-logit and auto-tuned thresholds corresponds to our previous approach, ContMAV. Results are shown in Tab. 13. Notice how, without using the pre-logit, using the learned thresholds achieves extremely similar performance to not using them. This result is expected as in our previous paper we had an intensive phase of hyperparameter tuning (discussed in the supplementary material of the related paper [75]) to achieve optimal performance. In this case, without any tuning we managed

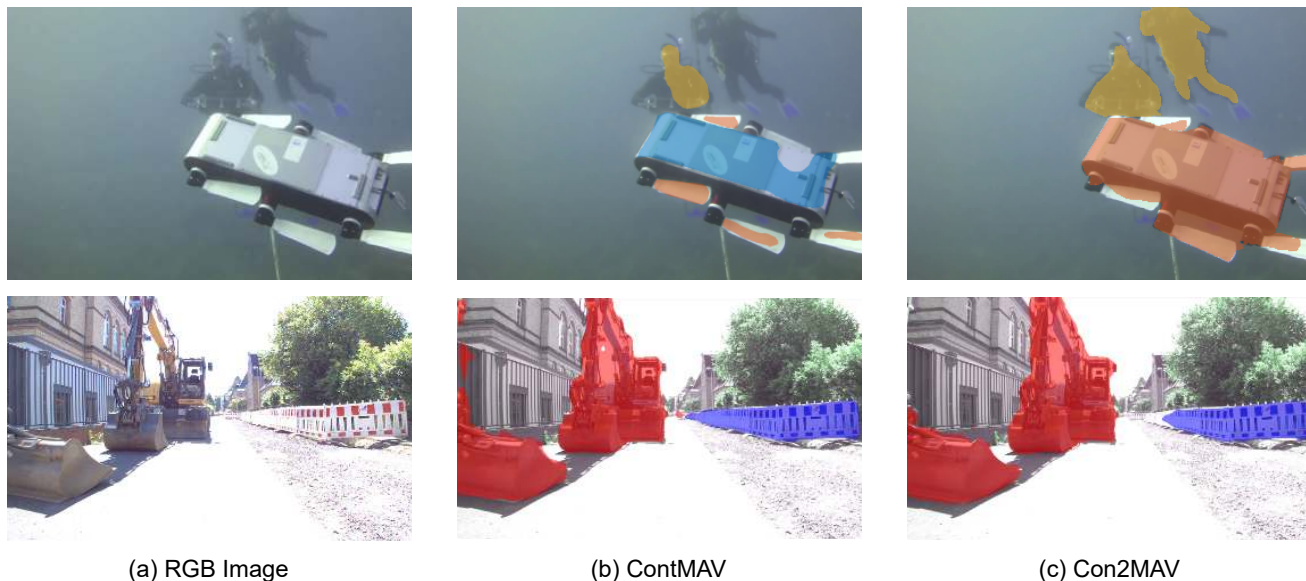


Fig. 5. Qualitative results of our approach, Con2MAV, on open-world semantic segmentation on SUIM (top row) and PANIC (bottom row). The prediction mask is overlaid to the input RGB for clarity. In the prediction, different colors correspond to different predicted classes. We compare our approach, Con2MAV (right), with our old method, ContMAV (center).



Fig. 6. Qualitative results of our approach, Con2MAV, on open-set panoptic segmentation on COCO (top row), and PANIC (bottom row). The prediction mask is overlaid to the input RGB for clarity. In the semantic prediction, the colored area indicates the anomalous region. In the instance prediction, different colors correspond to different instance ids.

to get similar performance for both mIoU and panoptic quality. The use of pre-logit instead of pre-softmax boosts performance by 4 – 5% on both metrics. The learned thresholds bring a further improvement when paired with the pre-logit, probably because the class descriptors are more robust and the post-processing manages to better separate the newly-discovered classes.

The second ablation study investigates the loss functions we used for class-agnostic instance segmentation. We compare our full model with one lacking both divergence and curl, and the two variants in which only one of the two vector field inspired loss functions is used. Results are shown in Tab. 14. Notice how the mIoU is always highly similar. This is expected since these loss functions do not have any impact on the semantic segmentation. The small differences are due to the fact that they all affect the shared encoder through backpropagation. However, changes are not significant. The use of either divergence or curl already improves performance on instance segmentation, when compared

to an approach that only uses the standard offset loss. Additionally, the experiment suggests that divergence is more useful than curl for instance segmentation, when considered individually. Combining the two proves to be the best possible combination.

7 LIMITATIONS AND FUTURE WORK

In this article, we formalized the task of open-world panoptic segmentation, and proposed the first approach that tackles it, as well as the first benchmark that allows a compelling evaluation of the task in the autonomous driving domain. As shown in the various experiments, our approach achieves state-of-the-art results on several datasets on all kinds of open-world segmentation tasks (see Sec. 3). An important takeaway of our method is that the pre-logit features we use seem to be more robust and reliable than the pre-softmax features we used in our previous work [75]. Pre-logits, in fact, yield competitive performance independently

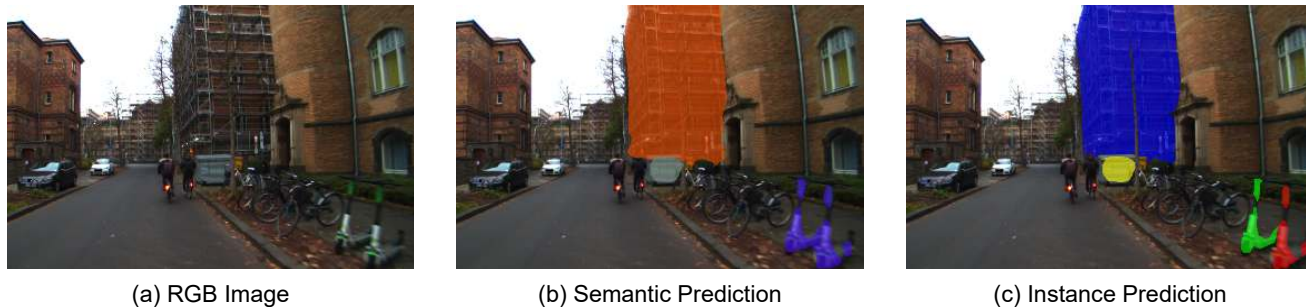


Fig. 7. Qualitative results of our approach, Con2MAV, on open-world panoptic segmentation on PANIC. The prediction mask is overlaid to the input RGB for clarity. In the semantic prediction, different colors correspond to different predicted classes. In the instance prediction, different colors correspond to different instance ids.

K %	Approach	Unknown Classes		
		PQ _{unk} [%] ↑	SQ _{unk} [%] ↑	RQ _{unk} [%] ↑
5	Void-train	8.6	72.7	11.8
	EOPSN [34]	23.1	74.7	30.9
	Mask2Anomaly [65]	24.3	78.2	32.1
	Con2MAV (ours)	25.1	78.4	34.6
10	Void-train	8.1	72.6	11.2
	EOPSN [34]	17.9	76.8	23.3
	Mask2Anomaly [65]	19.7	77.0	25.7
	Con2MAV (ours)	21.3	77.1	27.6
20	Void-train	7.5	72.9	10.3
	EOPSN [34]	11.3	73.8	15.3
	Mask2Anomaly [65]	14.6	76.2	19.1
	Con2MAV (ours)	22.1	88.5	24.9

TABLE 10. Open-set panoptic segmentation results on the COCO validation set on three different known-unknown splits. K denotes the percentage of unknown classes present in the dataset. Best results are highlighted in bold.

Approach	Unknown Classes		
	PQ _{unk} [%] ↑	SQ _{unk} [%] ↑	RQ _{unk} [%] ↑
Con2MAV (ours)	21.6	72.4	28.4

TABLE 11. Open-set panoptic segmentation results on the hidden test set of our dataset, PANIC. Public competition is available at <https://www.codabench.org/competitions/4562>.

from the dataset domain, number of known categories, number of unknown categories to discover, and type of open-world task. Still, our approach presents some limitations which offer interesting avenues for future work to increase robustness and performance.

The main limitation of our approach is that it relies on what Bendale et al. [4] called the “known unknown”, i.e., those areas of the training set that fall into the void/unlabeled portion of the image because they do not belong to any known category. We leverage these areas in the contrastive decoder to train the object-sphere loss and robustify our anomaly segmentation. Thus, our approach would suffer from a fully-labeled dataset, where no pixel is left with no ground truth annotation. An intuitive solution to this could be to choose a few classes from the known categories and treat them as known unknowns. On one hand, this would enable open-world segmentation and allow us to discover novel classes at training time, but on the other hand we would harm segmentation performance on the chosen classes. However, this approach would not be useful on datasets that have only few known categories [84], where discarding even just one of them would make the training set collapse to just a few samples. Another way to address this

problem is to introduce out-of-distribution data to the training set, which is a common strategy in literature [17], [25], [56].

Also, our approach leverages a post-processing operation which slows down the end-to-end approach, hindering real-time performance. This limitation we share with all approaches performing panoptic segmentation using offset or embeddings to predict instances. A possible solution would be to follow the paradigm of transformer-based architectures that get rid of the post-processing operation to directly predict masks for the individual objects [13]. However, these approaches has its own potential drawbacks, such as considerably longer training time, and the necessity to fix the number of object masks that can be predicted, while we can predict a virtually unlimited number of anomalies.

Interesting research avenues lie in the extension of our approach to other sensor modalities and other tasks. Since our contribution does not include any architectural change, but it resides in loss functions and training techniques, it would be interesting to apply it to open-world segmentation on, for example, RGB-D frames or LiDAR point clouds. Despite datasets for open-world segmentation are not common in the RGB-D domain, the SemanticKITTI dataset [3] already provides a competition for open-world segmentation on LiDAR point clouds. Similarly, our insights can be applied to approaches for object tracking. We believe that this will become a prominent problem, especially in the autonomous driving context, where tracking a moving object, despite not knowing what it is, is important for safety reasons.

Our benchmark, PANIC, is the first test set that allows the evaluation of open-world panoptic segmentation task. Extensive experiments show that our benchmark seem to be more challenging than other datasets commonly used in the literature, for which many approaches yield close-to-perfect performance [10]. As discussed, for designing PANIC we consider all classes annotated in Cityscapes as known, and aim to discover all others. The main limitation of our dataset, which is an interesting research direction for us, is that it does not provide annotation for the known categories. We only evaluate how good the anomalous classes and objects are segmented. This limitation we share with other benchmarks specifically designed for open-world tasks, such as SegmentMeIfYouCan [10] and Fishyscapes [7], but we believe it provides an interesting future work to address in order to be able to comprehensively evaluate global segmentation performance.

Finally, we note that open-world panoptic segmentation is closely related to another research direction, namely open-vocabulary segmentation. Open-vocabulary approaches also tackle the problem of segmenting novel classes and objects, but they do so by using language models that enable class discovery. As

Approach	Unknown Classes					
	PQ [%] \uparrow	SQ [%] \uparrow	RQ [%] \uparrow	mIoU _{unk} [%] \uparrow	Completeness [%] \uparrow	Homogeneity [%] \uparrow
Con2MAV (ours)	25.1	46.8	28.8	20.2	77.6	78.3

TABLE 12. Open-world panoptic segmentation results on the hidden test set of our dataset, PANIC. Public competition is available at <https://www.codabench.org/competitions/4477>.

Pre-Logit	Learned Th.	Unknown Classes	
		mIoU [%] \uparrow	PQ [%] \uparrow
		50.3	14.4
\checkmark		54.7	19.2
	\checkmark	50.2	15.8
\checkmark	\checkmark	57.3	22.4

TABLE 13. Ablation study to show the individual contribution of applying the MAV loss to the pre-logit layer, and of the learned thresholds. The last row corresponds to our approach, Con2MAV.

Offset	Divergence	Curl	Unknown Classes	
			mIoU [%] \uparrow	PQ [%] \uparrow
\checkmark			57.1	12.4
\checkmark	\checkmark		56.7	17.8
\checkmark		\checkmark	56.9	15.0
\checkmark	\checkmark	\checkmark	57.3	22.4

TABLE 14. Ablation study to investigate the ability to generalize to unknown objects of the loss functions used for segmenting instances. The last row corresponds to our approach, Con2MAV.

discussed in Sec. 2, in this work we do not use any language model and keep the task purely based on visual perception.

8 CONCLUSION

In this work, we introduce Con2MAV, the first approach for open-world panoptic segmentation, and PANIC, a new benchmark for several open-world segmentation tasks in the autonomous driving domain. Through extensive quantitative experiments on multiple datasets, we demonstrate the effectiveness on Con2MAV across different domains (autonomous driving, everyday scenes, underwater monitoring) on all four tasks we introduce. Furthermore, our experiments on PANIC show how challenging the proposed dataset is. We believe this work, and especially the creation of a dedicated benchmark for all kinds of open-world segmentation tasks, will pave the way to the development of novel approaches and encourage further advancements in the field.

ACKNOWLEDGMENTS

We thank Benedikt Mersch, Lucas Nunes, Ignacio Vizzo, and Louis Wiesmann for developing and taking care of the sensor platform used for recording the data. We thank Fares Hosn and Aibek Zurbayev for helping with labeling data. The work has been funded by the Deutsche Forschungsgemeinschaft (DFG, German Research Foundation) under Germany’s Excellence Strategy, EXC-2070 – 390732324 (PhenoRob), and by the German Federal Ministry of Education and Research (BMBF) in the project “Robotics Institute Germany”, grant No. 16ME0999.

REFERENCES

- [1] J. Ackermann, C. Sakaridis, and F. Yu, “Maskomaly: Zero-shot mask anomaly segmentation,” in *Proc. of British Machine Vision Conference (BMVC)*, 2023. 10
- [2] J. T. Barron, “A General and Adaptive Robust Loss Function,” in *Proc. of the IEEE/CVF Conf. on Computer Vision and Pattern Recognition (CVPR)*, 2019. 7
- [3] J. Behley, M. Garbade, A. Milioto, J. Quenzel, S. Behnke, C. Stachniss, and J. Gall, “SemanticKITTI: A Dataset for Semantic Scene Understanding of LiDAR Sequences,” in *Proc. of the IEEE/CVF Intl. Conf. on Computer Vision (ICCV)*, 2019. 13
- [4] A. Bendale and T. E. Boult, “Towards open set deep networks,” in *Proc. of the IEEE Conf. on Computer Vision and Pattern Recognition (CVPR)*, 2016. 2, 8, 13
- [5] P. Bergmann, M. Fauser, D. Sattlegger, and C. Steger, “MVTec AD—A comprehensive real-world dataset for unsupervised anomaly detection,” in *Proc. of the IEEE/CVF Conf. on Computer Vision and Pattern Recognition (CVPR)*, 2019. 3
- [6] H. Blum, P. E. Sarlin, J. Nieto, R. Siegwart, and C. Cadena, “Fishyscapes: A benchmark for safe semantic segmentation in autonomous driving,” in *Proc. of the IEEE/CVF Conf. on Computer Vision and Pattern Recognition Workshops*, 2019. 3, 8
- [7] H. Blum, P. E. Sarlin, J. Nieto, R. Siegwart, and C. Cadena, “The Fishyscapes Benchmark: Measuring blind spots in semantic segmentation,” *Intl. Journal of Computer Vision (IJCV)*, vol. 129, pp. 3119–3135, 2021. 1, 2, 10, 13, 18
- [8] S. Borse, Y. Wang, Y. Zhang, and F. Porikli, “Inverseform: A loss function for structured boundary-aware segmentation,” in *Proc. of the IEEE/CVF Conf. on Computer Vision and Pattern Recognition (CVPR)*, 2021. 2
- [9] D. O. Cardoso, J. Gama, and F. M. França, “Weightless neural networks for open set recognition,” *Machine Learning*, vol. 106, no. 9-10, pp. 1547–1567, 2017. 2
- [10] R. Chan, K. Lis, S. Uhlemeyer, H. Blum, S. Honari, R. Siegwart, P. Fua, M. Salzmann, and M. Rottmann, “SegmentMeIfYouCan: A Benchmark for Anomaly Segmentation,” in *Proc. of the Conf. on Neural Information Processing Systems (NeurIPS)*, 2021. 1, 2, 3, 4, 7, 8, 9, 13, 19
- [11] T. Chen, S. Kornblith, M. Norouzi, and G. Hinton, “A Simple Framework for Contrastive Learning of Visual Representations,” in *Proc. of the Intl. Conf. on Machine Learning (ICML)*, 2020. 6, 10, 17
- [12] B. Cheng, M. D. Collins, Y. Zhu, T. Liu, T. S. Huang, H. Adam, and L.-C. Chen, “Panoptic-DeepLab: A Simple, Strong, and Fast Baseline for Bottom-Up Panoptic Segmentation,” in *Proc. of the IEEE/CVF Conf. on Computer Vision and Pattern Recognition (CVPR)*, 2020. 1
- [13] B. Cheng, I. Misra, A. G. Schwing, A. Kirillov, and R. Girdhar, “Masked-attention mask transformer for universal image segmentation,” in *Proc. of the IEEE/CVF Conf. on Computer Vision and Pattern Recognition (CVPR)*, 2022. 1, 13
- [14] F. Chollet, “Xception: Deep learning with depthwise separable convolutions,” in *cvpr*, 2017. 4
- [15] T. A. Ciarfuglia, I. M. Motoi, L. Saraceni, M. Fawakherji, A. Sanfeliu, and D. Nardi, “Weakly and semi-supervised detection, segmentation and tracking of table grapes with limited and noisy data,” *Computers and Electronics in Agriculture*, vol. 205, p. 107624, 2023. 2
- [16] M. Cordts, M. Omran, S. Ramos, T. Rehfeld, M. Enzweiler, R. Benenson, U. Franke, S. Roth, and B. Schiele, “The Cityscapes dataset for semantic urban scene understanding,” in *Proc. of the IEEE Conf. on Computer Vision and Pattern Recognition (CVPR)*, 2016. 1, 3, 4, 7, 8
- [17] A. Delić, M. Grcić, and S. Segvić, “Outlier detection by ensembling uncertainty with negative objectness,” *arXiv preprint*, vol. arXiv:2402.15374, 2024. 1, 10, 13
- [18] T. DeVries and G. W. Taylor, “Learning confidence for out-of-distribution detection in neural networks,” *arXiv preprint*, vol. arXiv:1802.04865, 2018. 10
- [19] A. R. Dhamija, M. Günther, and T. Boult, “Reducing network agnostophobia,” in *Proc. of the Conf. on Neural Information Processing Systems (NeurIPS)*, 2018. 2, 6, 17

- [20] M. Everingham, L. Van Gool, C. K. Williams, J. Winn, and A. Zisserman, "The pascal visual object classes (voc) challenge," *Intl. Journal of Computer Vision (IJCV)*, vol. 88, pp. 303–338, 2010. **9**
- [21] Y. Gal and Z. Ghahramani, "Dropout as a Bayesian Approximation: Representing model uncertainty in deep learning," in *Proc. of the Intl. Conf. on Machine Learning (ICML)*, 2016. **2, 10**
- [22] S. Gasperini, A. Marcos-Ramiro, M. Schmidt, N. Navab, B. Busam, and F. Tombari, "Segmenting known objects and unseen unknowns without prior knowledge," in *Proc. of the IEEE/CVF Intl. Conf. on Computer Vision (ICCV)*, 2023. **2**
- [23] G. Ghiasi, X. Gu, Y. Cui, and T.-Y. Lin, "Scaling open-vocabulary image segmentation with image-level labels," in *Proc. of the Europ. Conf. on Computer Vision (ECCV)*, 2022. **3**
- [24] R. Girshick, "Fast R-CNN," in *Proc. of the IEEE Intl. Conf. on Computer Vision (ICCV)*, 2015. **1**
- [25] M. Grcić, P. Bevandić, and S. Segvić, "Densehybrid: Hybrid anomaly detection for dense open-set recognition," in *Proc. of the Europ. Conf. on Computer Vision (ECCV)*, 2022. **10, 13**
- [26] M. Grcić, J. Sarić, and S. Segvić, "On advantages of mask-level recognition for outlier-aware segmentation," in *Proceedings of the IEEE/CVF Conference on Computer Vision and Pattern Recognition*, 2023. **1**
- [27] S. Halligan, D. G. Altman, and S. Mallett, "Disadvantages of using the area under the receiver operating characteristic curve to assess imaging tests: a discussion and proposal for an alternative approach," *European Radiology*, vol. 25, pp. 932–939, 2015. **8**
- [28] K. He, G. Gkioxari, P. Dollár, and R. Girshick, "Mask r-cnn," in *Proc. of the IEEE/CVF Intl. Conf. on Computer Vision (ICCV)*, 2017. **1**
- [29] K. He, X. Zhang, S. Ren, and J. Sun, "Deep residual learning for image recognition," in *Proc. of the IEEE Conf. on Computer Vision and Pattern Recognition (CVPR)*, 2016. **4**
- [30] D. Hendrycks, S. Basart, M. Mazeika, A. Zou, J. Kwon, M. Mostajabi, J. Steinhardt, and D. Song, "Scaling out-of-distribution detection for real-world settings," *Proc. of the Intl. Conf. on Machine Learning (ICML)*, 2022. **1, 2, 3, 8, 9, 10, 19**
- [31] D. Hendrycks and K. Gimpel, "A baseline for detecting misclassified and out-of-distribution examples in neural networks," in *Proc. of the Intl. Conf. on Learning Representations (ICLR)*, 2017. **2, 10, 18**
- [32] W. Hu, H. Zhao, L. Jiang, J. Jia, and T.-T. Wong, "Bidirectional projection network for cross dimension scene understanding," in *Proc. of the IEEE/CVF Conf. on Computer Vision and Pattern Recognition (CVPR)*, 2021. **2**
- [33] G. Humblot-Renaux, S. Escalera, and T. B. Moeslund, "Beyond auROC & co. for evaluating out-of-distribution detection performance," in *Proc. of the IEEE/CVF Conf. on Computer Vision and Pattern Recognition (CVPR)*, 2023. **8**
- [34] J. Hwang, S. W. Oh, J.-Y. Lee, and B. Han, "Exemplar-based open-set panoptic segmentation network," in *Proc. of the IEEE/CVF Conf. on Computer Vision and Pattern Recognition (CVPR)*, 2021. **2, 4, 13**
- [35] M. J. Islam, C. Edge, Y. Xiao, P. Luo, M. Mehtaz, C. Morse, S. S. Enan, and J. Sattar, "Semantic segmentation of underwater imagery: Dataset and benchmark," in *Proc. of the IEEE/RSJ Intl. Conf. on Intelligent Robots and Systems (IROS)*, 2020. **1, 2, 9, 11, 20**
- [36] C. Jia, Y. Yang, Y. Xia, Y.-T. Chen, Z. Parekh, H. Pham, Q. Le, Y.-H. Sung, Z. Li, and T. Duerig, "Scaling up visual and vision-language representation learning with noisy text supervision," in *Proc. of the Intl. Conf. on Machine Learning (ICML)*, 2021. **3**
- [37] D. Kingma and J. Ba, "Adam: A Method for Stochastic Optimization," in *Proc. of the Intl. Conf. on Learning Representations (ICLR)*, 2015. **10**
- [38] A. Kirillov, R. Girshick, K. He, and P. Dollár, "Panoptic feature pyramid networks," in *Proc. of the IEEE/CVF Conf. on Computer Vision and Pattern Recognition (CVPR)*, 2019. **1**
- [39] A. Kirillov, K. He, R. Girshick, C. Rother, and P. Dollár, "Panoptic segmentation," in *Proc. of the IEEE/CVF Conf. on Computer Vision and Pattern Recognition (CVPR)*, 2019. **9**
- [40] S. Kong and D. Ramanan, "Opengan: Open-set recognition via open data generation," in *Proc. of the IEEE/CVF Conf. on Computer Vision and Pattern Recognition (CVPR)*, 2021. **3**
- [41] A. Kundu, X. Yin, A. Fathi, D. Ross, B. Brewington, T. Funkhouser, and C. Pantofaru, "Virtual multi-view fusion for 3d semantic segmentation," in *Proc. of the Europ. Conf. on Computer Vision (ECCV)*, 2020. **2**
- [42] B. Lakshminarayanan, A. Pritzel, and C. Blundell, "Simple and scalable predictive uncertainty estimation using deep ensembles," *Proc. of the Conf. on Neural Information Processing Systems (NeurIPS)*, 2017. **2**
- [43] F. Liang, B. Wu, X. Dai, K. Li, Y. Zhao, H. Zhang, P. Zhang, P. Vajda, and D. Marculescu, "Open-vocabulary semantic segmentation with mask-adapted clip," in *Proc. of the IEEE/CVF Conf. on Computer Vision and Pattern Recognition (CVPR)*, 2023. **3**
- [44] T.-Y. Lin, M. Maire, S. Belongie, J. Hays, P. Perona, D. Ramanan, P. Dollár, and C. L. Zitnick, "Microsoft COCO: Common objects in context," in *Proc. of the Europ. Conf. on Computer Vision (ECCV)*, 2014. **1, 2, 3, 9, 18, 20, 21**
- [45] S. Liu, L. Qi, H. Qin, J. Shi, and J. Jia, "Path aggregation network for instance segmentation," *Proc. of the IEEE/CVF Conf. on Computer Vision and Pattern Recognition (CVPR)*, 2018. **2**
- [46] W. Liu, X. Wang, J. Owens, and Y. Li, "Energy-based out-of-distribution detection," in *Proc. of the Conf. on Neural Information Processing Systems (NeurIPS)*, 2020. **2**
- [47] Y. Liu, I. E. Zulfikar, J. Luiten, A. Dave, D. Ramanan, B. Leibe, A. Osep, and L. Leal-Taixé, "Opening up open world tracking," in *Proc. of the IEEE/CVF Conf. on Computer Vision and Pattern Recognition (CVPR)*, 2022. **3**
- [48] J. Long, E. Shelhamer, and T. Darrell, "Fully convolutional networks for semantic segmentation," in *Proc. of the IEEE Conf. on Computer Vision and Pattern Recognition (CVPR)*, 2015. **1**
- [49] K. Maag and T. Riedlinger, "Pixel-wise gradient uncertainty for convolutional neural networks applied to out-of-distribution segmentation," in *Intl. Conf. on Computer Vision Theory and Applications (VISAPP)*, 2024. **2**
- [50] E. Marks, M. Sodano, F. Magistri, L. Wiesmann, D. Desai, R. Marcuzzi, J. Behley, and C. Stachniss, "High precision leaf instance segmentation for phenotyping in point clouds obtained under real field conditions," *IEEE Robotics and Automation Letters (RA-L)*, vol. 8, pp. 4791–4798, 2023. **1, 2**
- [51] L. McInnes, J. Healy, S. Astels *et al.*, "HDBScan: Hierarchical density based clustering," *Journal of Open Source Software*, vol. 2, p. 205, 2017. **7**
- [52] A. Milioto, L. Mandtler, and C. Stachniss, "Fast Instance and Semantic Segmentation Exploiting Local Connectivity, Metric Learning, and One-Shot Detection for Robotics," in *Proc. of the IEEE Intl. Conf. on Robotics & Automation (ICRA)*, 2019. **2**
- [53] A. Milioto and C. Stachniss, "Bonnet: An Open-Source Training and Deployment Framework for Semantic Segmentation in Robotics using CNNs," in *Proc. of the IEEE Intl. Conf. on Robotics & Automation (ICRA)*, 2019. **1, 2**
- [54] A. Milioto, P. Lottes, and C. Stachniss, "Real-time Semantic Segmentation of Crop and Weed for Precision Agriculture Robots Leveraging Background Knowledge in CNNs," in *Proc. of the IEEE Intl. Conf. on Robotics & Automation (ICRA)*, 2018. **2**
- [55] N. Mor and L. Wolf, "Confidence prediction for lexicon-free ocr," in *Proc. of the IEEE Winter Conf. on Applications of Computer Vision (WACV)*, 2018. **2**
- [56] N. Nayal, M. Yavuz, J. F. Henriques, and F. Güney, "Rba: Segmenting unknown regions rejected by all," in *Proc. of the IEEE/CVF Intl. Conf. on Computer Vision (ICCV)*, 2023. **1, 2, 10, 13**
- [57] A. Nekrasov, A. Hermans, L. Kuhnert, and B. Leibe, "Ugains: Uncertainty guided anomaly instance segmentation," in *Proc. of the German Conf. on Pattern Recognition (GCPR)*, 2023. **2**
- [58] A. Nekrasov, R. Zhou, M. Ackermann, A. Hermans, B. Leibe, and M. Rottmann, "Oodis: Anomaly instance segmentation benchmark," *arXiv preprint*, vol. arXiv:2406.11835, 2024. **3, 8**
- [59] D. Neven, B. D. Brabandere, M. Proesmans, and L. V. Gool, "Instance Segmentation by Jointly Optimizing Spatial Embeddings and Clustering Bandwidth," in *Proc. of the IEEE/CVF Conf. on Computer Vision and Pattern Recognition (CVPR)*, 2019. **6**
- [60] A. Nguyen, J. Yosinski, and J. Clune, "Deep neural networks are easily fooled: High confidence predictions for unrecognizable images," in *Proc. of the IEEE/CVF Conf. on Computer Vision and Pattern Recognition (CVPR)*, 2015. **2**
- [61] M. Orsic, I. Kreso, P. Bevandić, and S. Segvić, "In defense of pre-trained imagenet architectures for real-time semantic segmentation of road-driving images," in *Proc. of the IEEE/CVF Conf. on Computer Vision and Pattern Recognition (CVPR)*, 2019. **4**
- [62] P. Pinggera, S. Ramos, S. Gehrig, U. Franke, C. Rother, and R. Mester, "Lost and found: detecting small road hazards for self-driving vehicles," in *Proc. of the IEEE/RSJ Intl. Conf. on Intelligent Robots and Systems (IROS)*, 2016. **3**
- [63] J. Qin, J. Wu, P. Yan, M. Li, R. Yuxi, X. Xiao, Y. Wang, R. Wang, S. Wen, X. Pan *et al.*, "Freeseq: Unified, universal and open-vocabulary image segmentation," in *Proc. of the IEEE/CVF Conf. on Computer Vision and Pattern Recognition (CVPR)*, 2023. **3**
- [64] A. Radford, J. W. Kim, C. Hallacy, A. Ramesh, G. Goh, S. Agarwal, G. Sastry, A. Askell, P. Mishkin, J. Clark, G. Krueger, and I. Sutskever, "Learning transferable visual models from natural language supervision," in *Proc. of the Intl. Conf. on Machine Learning (ICML)*, 2021. **3**

- [65] S. N. Rai, F. Cermelli, B. Caputo, and C. Masone, "Mask2anomaly: Mask transformer for universal open-set segmentation," *IEEE Trans. on Pattern Analysis and Machine Intelligence (TPAMI)*, 2024. [1](#), [2](#), [4](#), [9](#), [13](#), [18](#)
- [66] S. Ren, K. He, R. Girshick, and J. Sun, "Faster r-cnn: Towards real-time object detection with region proposal networks," *IEEE Trans. on Pattern Analysis and Machine Intelligence (TPAMI)*, vol. 39, no. 6, pp. 1137–1149, 2016. [1](#)
- [67] G. Roggiolani, M. Sodano, T. Guadagnino, F. Magistri, J. Behley, and C. Stachniss, "Hierarchical approach for joint semantic, plant instance, and leaf instance segmentation in the agricultural domain," in *Proc. of the IEEE Intl. Conf. on Robotics & Automation (ICRA)*, 2023. [1](#), [2](#)
- [68] E. Romera, J. M. Alvarez, L. M. Bergasa, and R. Arroyo, "Erfnet: Efficient residual factorized convnet for real-time semantic segmentation," *IEEE Trans. on Intelligent Transportation Systems (ITS)*, vol. 19, no. 1, pp. 263–272, 2018. [4](#)
- [69] O. Ronneberger, P. Fischer, and T. Brox, "U-net: Convolutional networks for biomedical image segmentation," in *Proc. of the Intl. Conf. on Medical image computing and computer-assisted intervention (MICCAI)*, 2015. [4](#)
- [70] A. Rosenberg and J. Hirschberg, "V-measure: A Conditional Entropy-Based External Cluster Evaluation Measure," in *Proc. of the Joint Conf. on Empirical Methods in Natural Language Processing and Computational Natural Language Learning (EMNLP-CoNLL)*, 2007. [9](#)
- [71] M. Salehi, N. Sadjadi, S. Baselizadeh, M. H. Rohban, and H. R. Rabiee, "Multiresolution Knowledge Distillation for Anomaly Detection," in *Proc. of the IEEE/CVF Conf. on Computer Vision and Pattern Recognition (CVPR)*, 2021. [3](#)
- [72] H. Sapkota and Q. Yu, "Bayesian Nonparametric Submodular Video Partition for Robust Anomaly Detection," in *Proc. of the IEEE/CVF Conf. on Computer Vision and Pattern Recognition (CVPR)*, 2022. [2](#)
- [73] L. N. Smith and N. Topin, "Super-convergence: Very fast training of neural networks using large learning rates," in *Artificial Intelligence and Machine Learning for Multi-Domain Operations Applications*, vol. 11006, 2019, pp. 369–386. [10](#)
- [74] M. Sodano, F. Magistri, T. Guadagnino, J. Behley, and C. Stachniss, "Robust double-encoder network for rgb-d panoptic segmentation," in *Proc. of the IEEE Intl. Conf. on Robotics & Automation (ICRA)*, 2023. [1](#), [2](#)
- [75] M. Sodano, F. Magistri, L. Nunes, J. Behley, and C. Stachniss, "Open-world semantic segmentation including class similarity," in *Proc. of the IEEE/CVF Conf. on Computer Vision and Pattern Recognition (CVPR)*, 2024. [1](#), [2](#), [4](#), [5](#), [10](#), [11](#), [12](#), [17](#), [18](#), [19](#), [20](#)
- [76] C. Tang, H. Chen, X. Li, J. Li, Z. Zhang, and X. Hu, "Look closer to segment better: Boundary patch refinement for instance segmentation," in *Proc. of the IEEE/CVF Conf. on Computer Vision and Pattern Recognition (CVPR)*, 2021. [1](#)
- [77] T. Tommasi, N. Patricia, B. Caputo, and T. Tuytelaars, "A deeper look at dataset bias," *Domain Adaptation in Computer Vision Applications*, pp. 37–55, 2017. [2](#)
- [78] S. Vaze, K. Han, A. Vedaldi, and A. Zisserman, "Open-set recognition: A good closed-set classifier is all you need," in *Proc. of the Intl. Conf. on Learning Representations (ICLR)*, 2021. [2](#)
- [79] I. Vizzo, B. Mersch, L. Nunes, L. Wiesmann, T. Guadagnino, and C. Stachniss, "Toward reproducible version-controlled perception platforms: Embracing simplicity in autonomous vehicle dataset acquisition," in *Proc. of the IEEE Intl. Conf. on Intelligent Transportation Systems (ITSC)*, 2023. [1](#), [3](#), [8](#)
- [80] A. Vyas, N. Jammalamadaka, X. Zhu, D. Das, B. Kaul, and T. L. Willke, "Out-of-distribution detection using an ensemble of self supervised leave-out classifiers," in *Proc. of the Europ. Conf. on Computer Vision (ECCV)*, 2018. [2](#)
- [81] W. Wang, J. Dai, Z. Chen, Z. Huang, Z. Li, X. Zhu, X. Hu, T. Lu, L. Lu, H. Li, X. Wang, and Y. Qiao, "Internimage: Exploring large-scale vision foundation models with deformable convolutions," in *Proc. of the IEEE/CVF Conf. on Computer Vision and Pattern Recognition (CVPR)*, 2023. [2](#)
- [82] Z. Wang, Q. Xu, Z. Yang, Y. He, X. Cao, and Q. Huang, "Openauc: Towards auc-oriented open-set recognition," *Proc. of the Conf. on Neural Information Processing Systems (NeurIPS)*, 2022. [8](#)
- [83] J. Weyler, T. Läbe, J. Behley, and C. Stachniss, "Panoptic Segmentation with Partial Annotations for Agricultural Robots," *IEEE Robotics and Automation Letters (RA-L)*, vol. 9, no. 2, pp. 1660–1667, 2024. [5](#), [6](#), [7](#)
- [84] J. Weyler, F. Magistri, E. Marks, Y. L. Chong, M. Sodano, G. Roggiolani, N. Chebrolu, C. Stachniss, and J. Behley, "PhenoBench—A Large Dataset and Benchmarks for Semantic Image Interpretation in the Agricultural Domain," *IEEE Trans. on Pattern Analysis and Machine Intelligence (TPAMI)*, vol. 46, pp. 9583–9594, 2024. [1](#), [3](#), [13](#)
- [85] K. Wong, S. Wang, M. Ren, M. Liang, and R. Urtasun, "Identifying unknown instances for autonomous driving," in *Proc. of the Conf. on Robot Learning (CoRL)*, 2020. [2](#)
- [86] X. Xu, T. Xiong, Z. Ding, and Z. Tu, "Masclip for open-vocabulary universal image segmentation," in *Proc. of the IEEE/CVF Intl. Conf. on Computer Vision (ICCV)*, 2023. [3](#)
- [87] Z. Xu, S. Escalera, A. Pavão, M. Richard, W.-W. Tu, Q. Yao, H. Zhao, and I. Guyon, "Codabench: Flexible, easy-to-use, and reproducible meta-benchmark platform," *Patterns*, vol. 3, no. 7, p. 100543, 2022. [8](#), [18](#)
- [88] F. Yu, H. Chen, X. Wang, W. Xian, Y. Chen, F. Liu, V. Madhavan, and T. Darrell, "BDD100K: A diverse driving dataset for heterogeneous multitask learning," in *Proc. of the IEEE/CVF Conf. on Computer Vision and Pattern Recognition (CVPR)*, 2020. [3](#), [8](#)
- [89] O. Zendel, K. Honauer, M. Murschitz, D. Steininger, and G. F. Dominguez, "Wilddash-creating hazard-aware benchmarks," in *Proc. of the Europ. Conf. on Computer Vision (ECCV)*, 2018. [3](#)
- [90] H. Zhang, F. Li, X. Zou, S. Liu, C. Li, J. Yang, and L. Zhang, "A simple framework for open-vocabulary segmentation and detection," in *Proc. of the IEEE/CVF Intl. Conf. on Computer Vision (ICCV)*, 2023. [3](#)
- [91] H. Zhao, J. Shi, X. Qi, X. Wang, and J. Jia, "Pyramid Scene Parsing Network," in *Proc. of the IEEE/CVF Conf. on Computer Vision and Pattern Recognition (CVPR)*, 2017. [4](#)
- [92] Y. Zhao, "OmniAL: A Unified CNN Framework for Unsupervised Anomaly Localization," in *Proc. of the IEEE/CVF Conf. on Computer Vision and Pattern Recognition (CVPR)*, 2023. [3](#)



Matteo Sodano is a PhD student at the Photogrammetry & Robotics Lab at the University of Bonn since January 2021. He obtained his MSc degree in Control Engineering from "La Sapienza" University of Rome in 2020, with a thesis on motion planning for legged robots in collaboration with the Italian Institute of Technology (IIT). His research centers around perception and segmentation, with a focus on novel object discovery.



Federico Magistri is a Ph.D. student at the Photogrammetry Lab at the University of Bonn since November 2019. He has been a visiting student at the Centre for Robotics of the Queensland University of Technology in fall 2023. He received his M.Sc. in Artificial Intelligence and Robotics from "La Sapienza" University of Rome with a thesis on Swarm Robotics for Precision Agriculture in collaboration with the National Research Council of Italy and the Wageningen University and Research.



Jens Behley received his Dipl.-Inform. in computer science in 2009 and his Ph.D. in computer science in 2014, both from the Dept. of Computer Science at the University of Bonn, Germany. Since 2016, he is a postdoctoral researcher at the Photogrammetry & Robotics Lab at the University of Bonn, Germany. He finished his habilitation at the University of Bonn in 2023. His area of interest lies in the area of perception for autonomous vehicles, deep learning for semantic interpretation, and LiDAR-based SLAM.



Cyrill Stachniss is a full professor at the University of Bonn, Germany, with the University of Oxford, UK, as well as with the Lamarr Institute for Machine Learning and AI, Germany. He is the Spokesperson of the DFG Cluster of Excellence PhenoRob at the University of Bonn. His research focuses on probabilistic techniques and learning approaches for mobile robotics, perception, and navigation. Main application areas of his research are agricultural and service robotics and self-driving cars.

Open-World Panoptic Segmentation

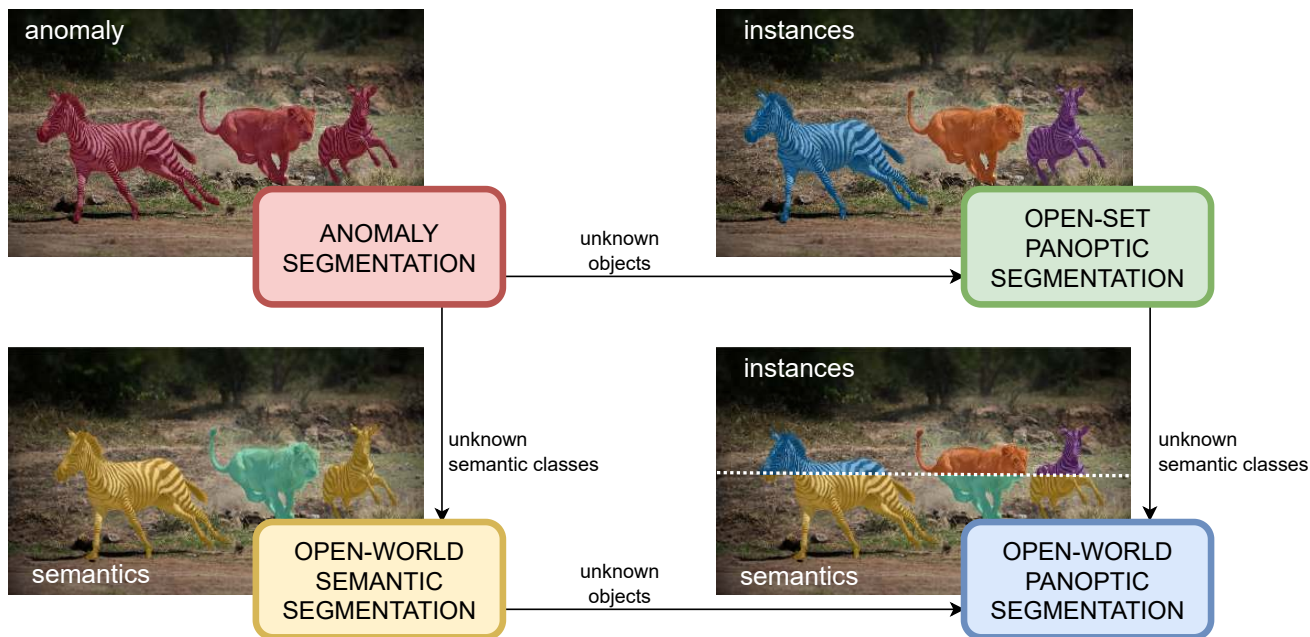


Fig. 8. A visual breakdown of the four open-world segmentation tasks discussed in this paper. Anomaly segmentation segment all anomalous areas as unknown (zebras and lion together). Open-world semantic segmentation separates classes but has no objects (zebras segmented together, lion separate). Open-set panoptic segmentation segment separate objects but has no information on having objects belonging to the same class. Open-world panoptic segmentation has both, classes and object information.

TASK DESCRIPTION

In Sec. 3 of the main paper, we propose a unique nomenclature for open-world segmentation tasks. Intuitively, anomaly segmentation is the task that aims to separate the unknown region from the known one, and has no knowledge of categories and object instances. The task of separating multiple categories only is called open-world semantic segmentation, while, in contrast, the task of segmenting object instances only is called open-set panoptic segmentation. Discovering both novel classes and objects is open-world panoptic segmentation. In Fig. 8, we show a visual example of the four task on an exemplary image that has been manually labeled for illustration purposes.

ADDITIONAL DETAILS ON THE CONTRASTIVE DECODER

As discussed in Sec. 4.2 of the main paper, in the paragraph dedicated to the contrastive decoder, we fix the radius of the hypersphere created by the objectsphere loss [19] to 1 (see Eq. (8) of the main paper). In principle, this hyperparameter could take any value. However, we pair the objectsphere loss to the contrastive loss [11], which aims to distribute all feature vectors on the unit sphere. Thus, we expect that any choice of the radius that is different from 1 would harm performance, since it would reduce the synergy between the two loss functions operating on the same decoder. In our previous work [75], we report an experiment about this. The general intuition is that when the radius of the hypersphere is $\xi < 1$, the performance is not dramatically harmed because the objectsphere loss aims to make the norm of the

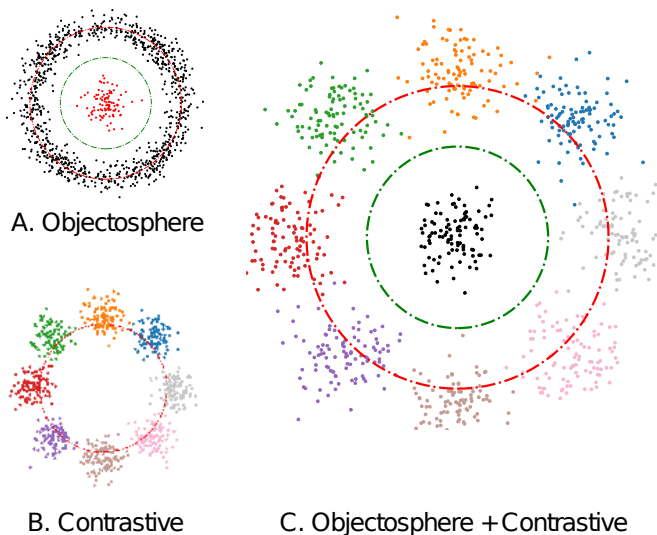


Fig. 9. A visual breakdown of the interaction between contrastive and objectsphere loss. The objectsphere loss is shown in A, where all points coming from known classes (black) lie around the red (outer) circle of radius ξ , and the points from unknown classes lie around the origin. The contrastive loss is shown in B, where features lie on the unit circle. Together, they lead to a behavior similar to the one depicted in C.

features belonging to the known pixels greater than ξ . Thus, the two losses do not work against each other. In contrast, when $\xi > 1$, the two loss functions try to achieve two tasks which

Approach	Unknown Classes					
	PQ [%] \uparrow	SQ [%] \uparrow	RQ [%] \uparrow	mIoU _{unk} [%] \uparrow	Completeness [%] \uparrow	Homogeneity [%] \uparrow
Con2MAV (ours)	22.4	44.9	39.5	19.9	74.8	77.9

TABLE 15. Open-world panoptic segmentation results on the validation set of PANIC.

Approach	Pixel-Level		Component-Level		
	AUPR [%] \uparrow	FPR95 [%] \downarrow	sIoU gt [%] \uparrow	PPV [%] \uparrow	mean F1 [%] \uparrow
ContMAV [75]	89.9	69.9	13.5	66.0	23.1
Con2MAV (ours)	92.2	50.1	18.9	59.9	28.4

TABLE 16. Anomaly segmentation results on the validation set of PANIC. Best results are highlighted in bold.

Approach	Unknown Classes		
	mIoU [%] \uparrow	Com [%] \uparrow	Hom [%] \uparrow
ContMAV [75]	15.3	84.3	84.2
Con2MAV (ours)	17.5	85.0	84.9

TABLE 17. Open-world semantic segmentation results on the validation set of PANIC. Best results are highlighted in bold.

are incompatible (features on the unit circle and, at the same time, with norm greater than 1), and performance suffers. In Fig. 9, we show a 2D visualization of the expected output of the contrastive decoder. The image has only illustrative purposes, and shows the ideal output in the 2D case. However, the feature vectors that the contrastive decoder predicts are D -dimensional, where D is the dimension of pre-logits features.

In our previous approach, we used K -dimensional features \mathbf{f} , where K was the number of known classes, and performed an experiment in order to verify whether the output of the decoder is aligned with our expectation. We define two thresholds ζ and ρ . Then, given \mathbf{f}_p^d , i.e., the feature predicted at pixel p from the contrastive decoder, we want $1 - \zeta < \|\mathbf{f}_p^d\|_2 < 1 + \zeta$ for all \mathbf{f}_p^d whose ground truth label is a known class, and $\|\mathbf{f}_p^d\|_2 < \rho$ for all \mathbf{f}_p^d whose ground truth label is an unknown class. The former means that the norms of the vectors belonging to known classes should be in a “tube” of radius ζ around 1, which is the radius of the hypersphere we selected. The latter means that the norms of the vectors belonging to unknown classes (which, at training time, are the unlabeled portions of the image), should be smaller than ρ . We chose $\zeta = 0.2$ and $\rho = 0.4$, and we find that 86.5% of the vectors belonging to known classes fall into the tube, and that 79.9% of the vectors belonging to unknown classes are smaller than ρ . This verifies that the output is aligned to our expectation.

To visually show the result, we would need to apply a dimensionality reduction approach such as principal component analysis. However, linear dimensionality reduction techniques always lead to loss of information, and the new dimensions may offer no concrete interpretability.

EXPERIMENTAL EVALUATION

In the following, we give details about the open-world splits for the COCO [44] dataset. Additionally, we report results on the validation set of our dataset, PANIC.

Approach	Unknown Classes		
	PQ _{unk} [%] \uparrow	SQ _{unk} [%] \uparrow	RQ _{unk} [%] \uparrow
Con2MAV (ours)	20.8	74.5	27.9

TABLE 18. Open-set panoptic segmentation results on the validation set of PANIC.

Approach	GFLOPs \downarrow	Training Parameters \downarrow
Maskomaly [31]	937	215M
Mask2Anomaly [7]	258	23M
ContMAV [75]	84	48M
Con2MAV (ours)	50	65M

TABLE 19. Architectural Efficiency

COCO Dataset for Open-World Segmentation Tasks

In the main paper, we used COCO [44] for several open-world segmentation tasks. For this, we followed the approach of Mask2Anomaly [65], and constructed open-world test sets by removing the labels of a small set of known classes from the training set. The removed set of classes are treated as unknown. We used three different training dataset split with increasing order of difficulty (5%, 10%, and 20% of unknown classes). The removed classes are removed cumulatively. For the 5% we removed “car”, “cow”, “pizza”, “toilet”. Additionally, for the 10% we removed “boat”, “tie”, “zebra”, “stop sign”. Finally, for the 20% we removed “dining table”, “banana”, “bicycle”, “cake”, “sink”, “cat”, “keyboard”, and “bear”.

Results on Validation Set of the PANIC Dataset

We mentioned in the main paper that PANIC is composed of a hidden test set and a validation set. In the experimental evaluation of the main paper, we report the evaluation on the hidden test set. Here, we use the same evaluation pipeline that we uploaded on Codabench [87] for the benchmark competitions to extract metrics on the validation data as well. Notice that results on the validation and the test set are completely independent, since no class that appears in the test set appears also in the validation set, in order to keep the test set truly hidden. However, validation set numbers are apparently good indicators of test set performance and, therefore, should ensure that insights on the validation set transfer well to the test set. We report open-world panoptic segmentation results on the validation set of PANIC in Tab. 15. Additionally, we also report results for anomaly segmentation in Tab. 16, open-world semantic segmentation in Tab. 17, and open-set panoptic segmentation in Tab. 18. As for the test set experiments in the main paper, we report both our old approach ContMAV (as baseline) and our current approach Con2MAV for anomaly and open-world semantic segmentation. The results are further evidence that we improved over our previous work.

ARCHITECTURAL EFFICIENCY

As pointed out in Sec. 4 of the main paper, we designed our neural network in order to be lightweight. In Tab. 19, we report the number of parameters and the GFLOPs of our model together with three state-of-the-art models with code available from the SegmentMeIfYouCan public benchmark. We show that our architecture is competitive and performs well in terms of efficiency.

QUALITATIVE RESULTS

In the following pages, we show qualitative results for anomaly segmentation in Fig. 10, open-world semantic segmentation in Fig. 11, open-set panoptic segmentation in Fig. 12, and open-world panoptic segmentation in Fig. 13 on various datasets. These results also show additional images from the PANIC benchmark we propose.

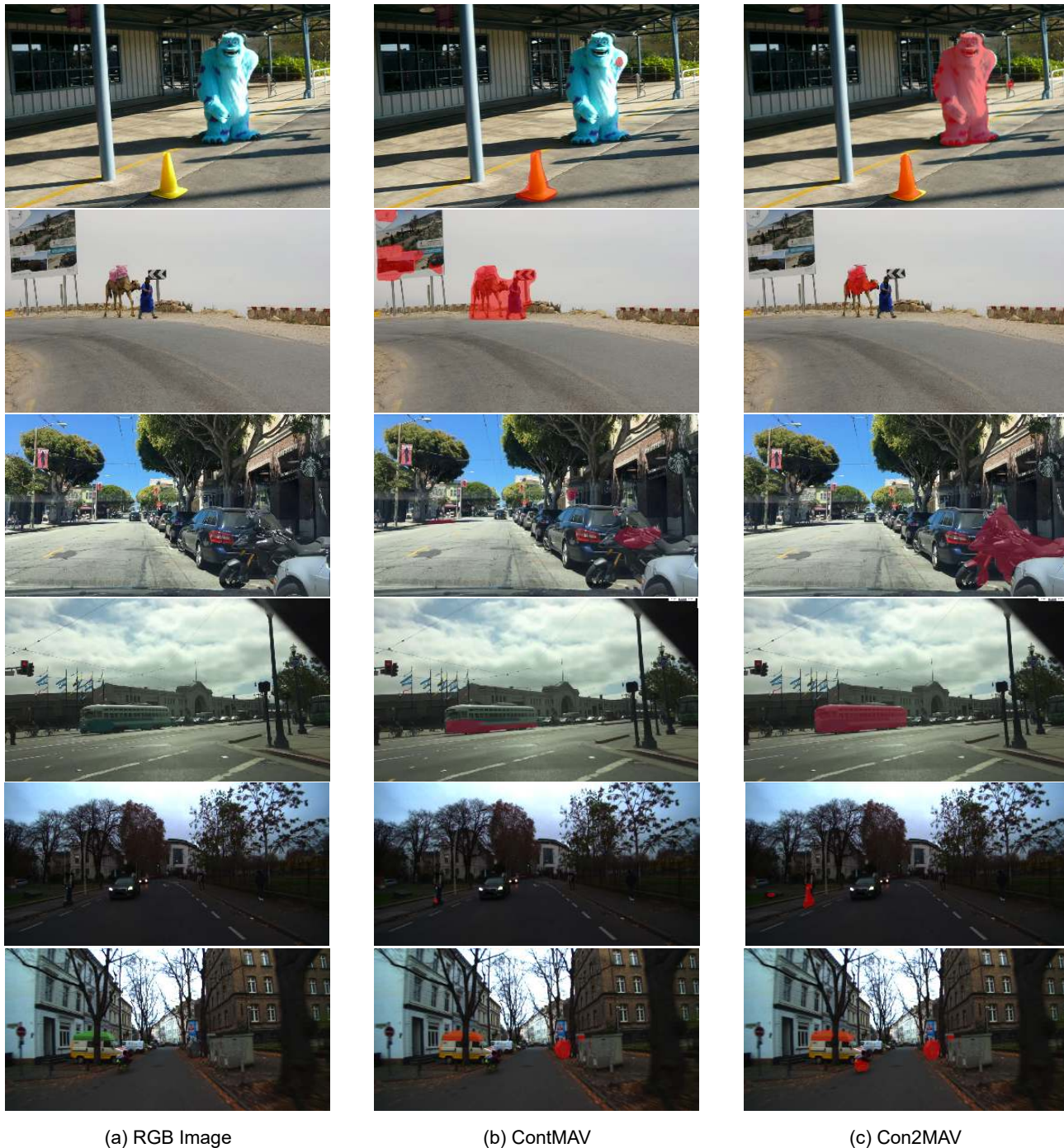


Fig. 10. Qualitative results on anomaly segmentation. We show the input RGB image on the left, the prediction of our previous approach ContMAV [75] in the middle, and the prediction of our current approach Con2MAV on the right. The top two images belong to SegmentMeIfYouCan [10], the middle two images belong to BDDAnomaly [30], the bottom two images belong to our dataset PANIC. In the prediction columns, we overlaid the prediction mask in red over the RGB image.

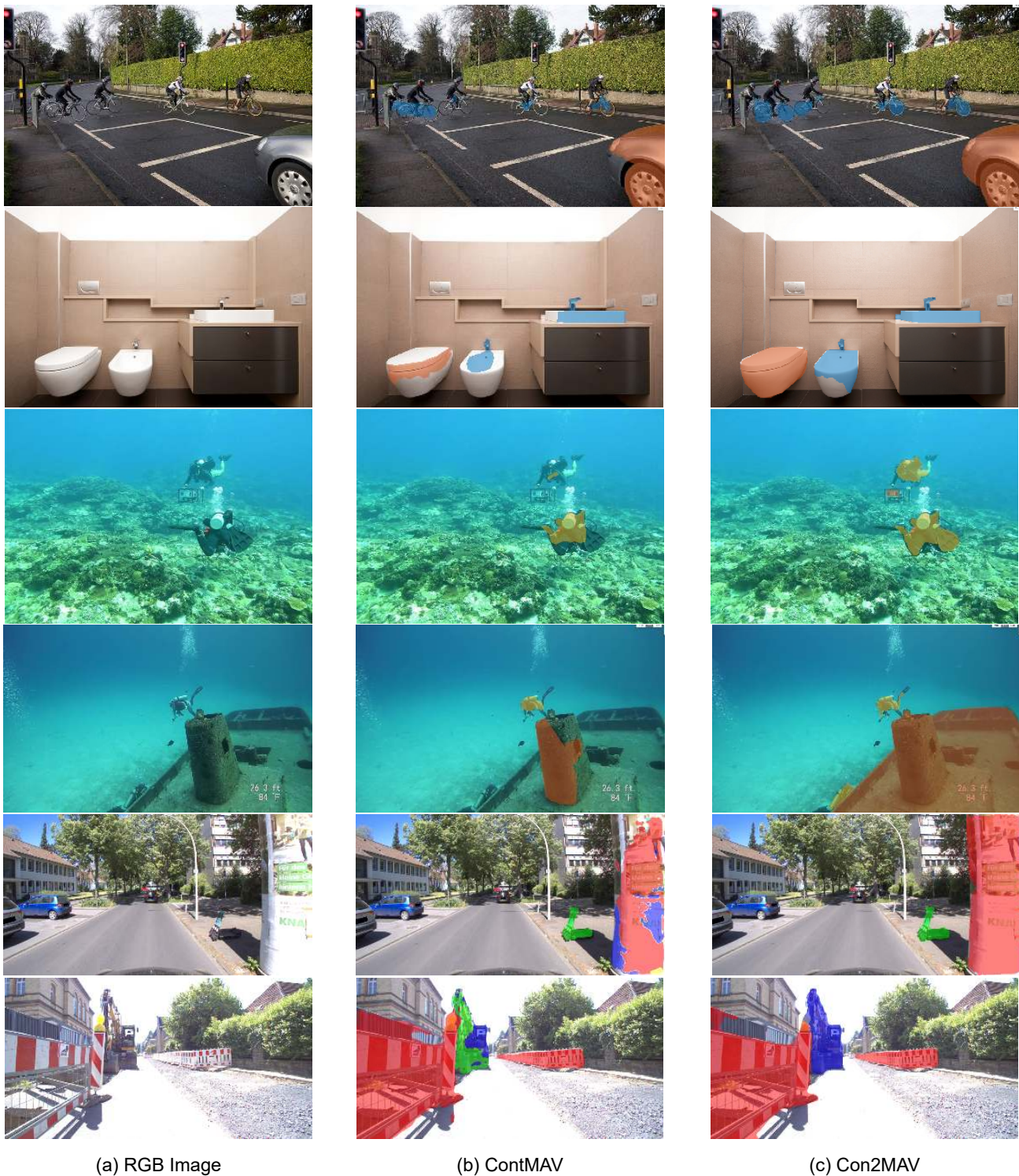


Fig. 11. Qualitative results on open-world semantic segmentation. We show the input RGB image on the left, the prediction of our previous approach ContMAV [75] in the middle, and the prediction of our current approach Con2MAV on the right. The top two images belong to COCO [44], the middle two images belong to SUIM [35], the bottom two images belong to our dataset PANIC. In the prediction columns, we overlaid the prediction mask over the RGB image. Different colors in the prediction correspond to different predicted categories.



Fig. 12. Qualitative results on open-set panoptic segmentation. We show the input RGB image on the left, the anomaly prediction of Con2MAV in the middle, and the instance prediction of Con2MAV on the right. The top three images belong to COCO [44], the bottom three images belong to our dataset PANIC. In the anomaly prediction, we overlaid the prediction mask over the RGB image in red. In the instance prediction, we overlaid the prediction mask over the RGB image in different colors, where different colors indicate different predicted instances.

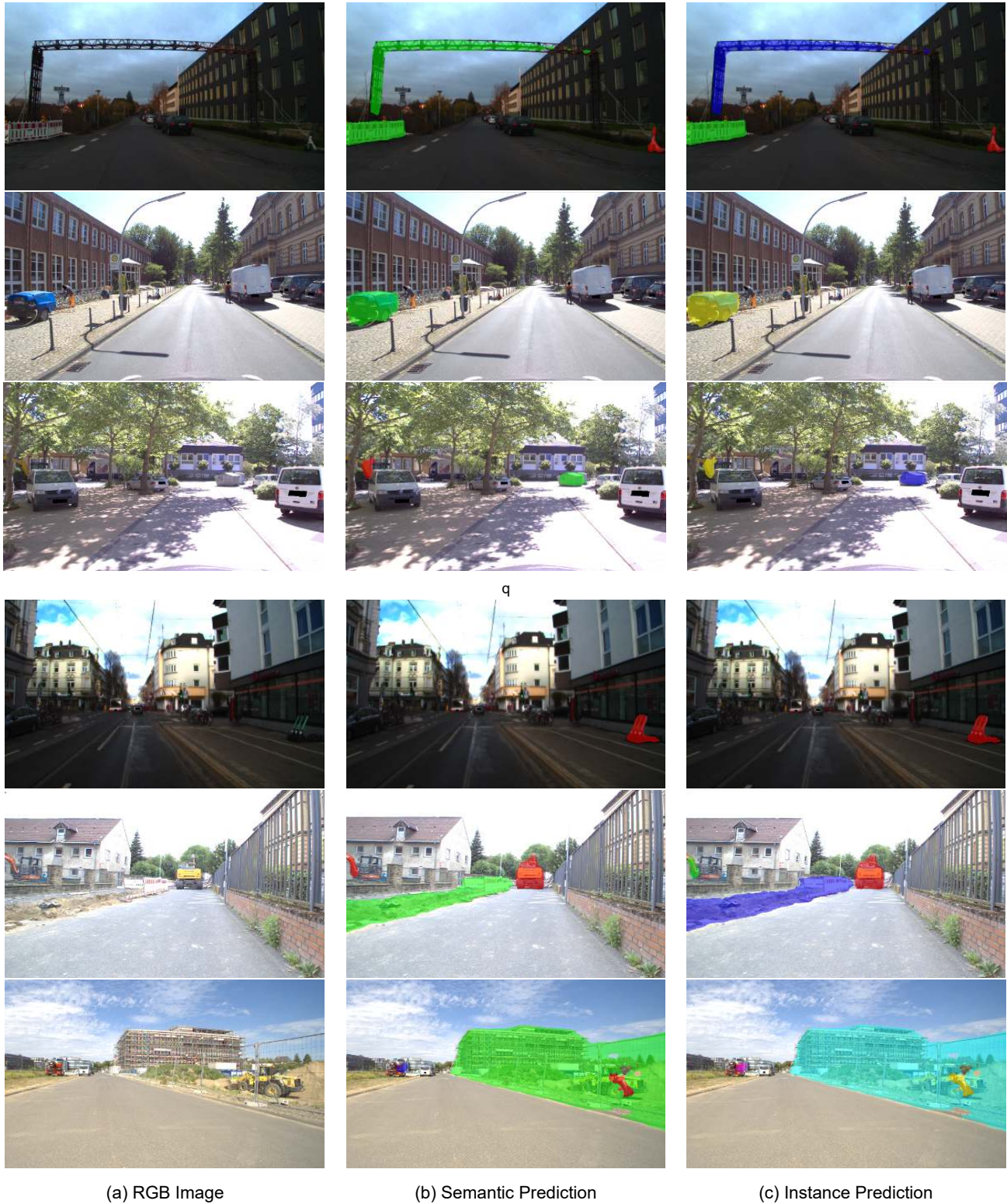


Fig. 13. Qualitative results on open-world panoptic segmentation. We show the input RGB image on the left, the open-world semantic prediction of Con2MAV in the middle, and the instance prediction of Con2MAV on the right. All six images belong to our dataset PANIC. In the semantic prediction, we overlaid the prediction mask over the RGB image in red, where different colors indicate different predicted categories. In the instance prediction, we overlaid the prediction mask over the RGB image in different colors, where different colors indicate different predicted instances.